NASA TechBriefs

National Aeronautics and Space Administration

99-02

February 1999

INTRODUCTION

Tech Briefs are short announcements of new technology derived from the research and development activities of the National Aeronautics and Space Administration. These Briefs emphasize information considered likely to be transferable across industrial, regional, or disciplinary lines and are issued to encourage commercial application.

Availability of NASA Tech Briefs and TSP's

Distribution of NASA Tech Briefs, a monthly periodical publication, is limited to engineers in U.S. Industry and to other domestic technology transfer agents. Requests for individual Tech Briefs or for Technical Support Packages (TSP's) announced herein should be addressed to

NASA Center for AeroSpace Information
Technology Transfer Office
800 Elkridge Landing Rd.
Linthicum Heights, MD 21090-2934
Telephone No. (301) 621-0245

Please reference the three-letter, five-digit control number located at the end of each Tech Brief. Information on NASA's Technology Utilization Program, its documents, and services is also available at the same facility.

Technology Utilization Officers and Patent Counsels are located at NASA field installations to provide technology-transfer access to industrial users. Inquiries can be made by writing to NASA field installations listed below.

Technology Utilization Officers and Patent Counsels

Ames Research Center
Technology Utilization Officer
Mail Code 223-3
Moffett Field, CA 94035

Patent Counsel
Mail Code 200-11
Moffett Field, CA 94035

Goddard Space Flight Center
Technology Utilization Officer
Mail Code 702-1
Greenbelt, MD 20771

Patent Counsel
Mail Code 204
Greenbelt, MD 20771

Lyndon B. Johnson Space Center
Technology Utilization Officer
Mail Code IC-4
Houston, TX 77058

Patent Counsel
Mail Code AL3
Houston, TX 77058

John F. Kennedy Space Center
Technology Utilization Officer
Mail Stop PT-PMO-A
Kennedy Space Center, FL 32899

Patent Counsel
Mail Code PT-PAT
Kennedy Space Center, FL 32899

Langley Research Center
Technology Utilization Officer
Mail Stop 143
Hampton, VA 23665

Patent Counsel
Mail Code 279
Hampton, VA 23665

Lewis Research Center
Technology Utilization Officer
Mail Stop 7-3
21000 Brookpark Road
Cleveland, OH 44135

Patent Counsel
Mail Code LE-LAW
21000 Brookpark Road
Cleveland, OH 44135

Jet Propulsion Laboratory
Technology Utilization Officer
Mail Stop 156-211
4800 Oak Grove Drive
Pasadena, CA 91109

NASA Resident Office-JPL
Technology Utilization Officer
Mail Stop 180-801
4800 Oak Grove Drive
Pasadena, CA 91109

Patent Counsel
Mail Code 180-801
4800 Oak Grove Drive
Pasadena, CA 91109

George C. Marshall Space Flight Center
Technology Utilization Officer
Code AT01
Marshall Space Flight Center, AL 35812

Patent Counsel
Mail Code CC01
Marshall Space Flight Center, AL 35812

John C. Stennis Space Center
Technology Utilization Officer
Code HA-30
Stennis Space Center, MS 39529

NASA Headquarters
Technology Utilization Officer
Code CU
Washington, DC 20546

Assistant General Counsel for Patent Matters
Code GP
Washington, DC 20546

Dryden Flight Research Center
Technology Utilization Officer
M/S D21-31
Bldg. 4832 Whse 7
Lilly Dr.
Edwards, CA 93523

BLANK PAGE

NASA TechBriefs

National Aeronautics and Space Administration

February 1999
99-02

BLANK PAGE

4

Electronic Components and Circuits

Hardware, Techniques, and Processes

BLANK PAGE

Using Surface-Plasmon Filters To Generate Scrolling Colors

Efficiencies of liquid-crystal display devices would be increased.

NASA's Jet Propulsion Laboratory, Pasadena, California

Surface-plasmon tunable filters (SPTFs) have been proposed for use in generating scrolling colors on the faces of liquid-crystal display (LCD) devices. In comparison with a conventional color LCD device equipped with primary-color filters, a LCD device equipped with SPTFs according to the proposal would utilize a greater proportion of the available luminous flux, generating a display about six times as bright, eliminate the in-pixel dye color filters, and cut number of pixels to one third.

A conventional color LCD device operates with linearly polarized light and is equipped with primary-color filters, there being a complete set of such filters (red, green, and blue) in each pixel. Therefore half the available white illumination is rejected through rejection of one of the polarization components. If one primary color is selected for display in a given pixel at a given time, then no more than about 1/3 of the remaining available illumination is utilized. Thus, only about 1/6 of the initially available illumination is utilized.

According to the proposal, white illumination for an entire LCD device would be processed through assemblies of SPTFs and prisms. The SPTFs would serve as polarization-sensitive band-pass filters to generate the primary colors, while the prisms would serve as total internal reflectors to change the direction of the light.

Incident unpolarized white light would enter the top assembly which contains three SPTFs. It would allow only p-polarized light to generate scrolling RGB (red, green, blue) colors and would reflect the remainder of the incident light downward to the bottom of assembly. For example, the very top SPTF would allow red color pass through only, the downward-reflected remainder of the incident light would be totally internally reflected toward the middle SPTF of the top assembly, which would only pass p-polarized green light. In a similar manner, the bottom SPTF of the top assembly would be made to pass only the p-polarized blue light and reflect the remaining light downward. At this point, the remaining downward-reflected light would comprise the s-polarized portion of the incident white light.

Using scrolling color, the frame should change three times faster, i.e., a 180-Hz frame rate is needed. For example, at the first 1/3 of the 1/60 second, the image on a black-and-white LCD screen would look like this: the sixth and the third sections are red, the fifth and the second sections are green, and the fourth and the first sections are blue. At the next moment, the second 1/3 of the 1/60 second, the colors scrolling downward, the image on the black-and-white LCD screen would look like this: the sixth and the third sections are blue, the fifth and the second sections are red, and the fourth and the first sections are green. At the last 1/3 of the 1/60 second, the image on the black-and-white LCD screen would look like this: the sixth and the third sections are green, the fifth and the second sections are blue, and the fourth and the first sections are red. Therefore, one sees a full color image at 60 Hz.

The bottom assembly would function similarly to the top assembly, except that it would be configured to receive the remaining downward-reflected light, and its SPTFs would be made perpendicular to those of the top assembly so as to exploit the s polarization of this light. Unlike in a conventional color LCD, the two assemblies would utilize both polarization components and all three color components of the white illumination. Thus, the display would be about 6 times as bright as is a conventional LCD.

During each third of a frame period, the voltage applied to each SPTF could be changed so as to change its pass wavelength band to that of a different primary color. The temporal sequence of voltages applied to the six SPTFs could be chosen

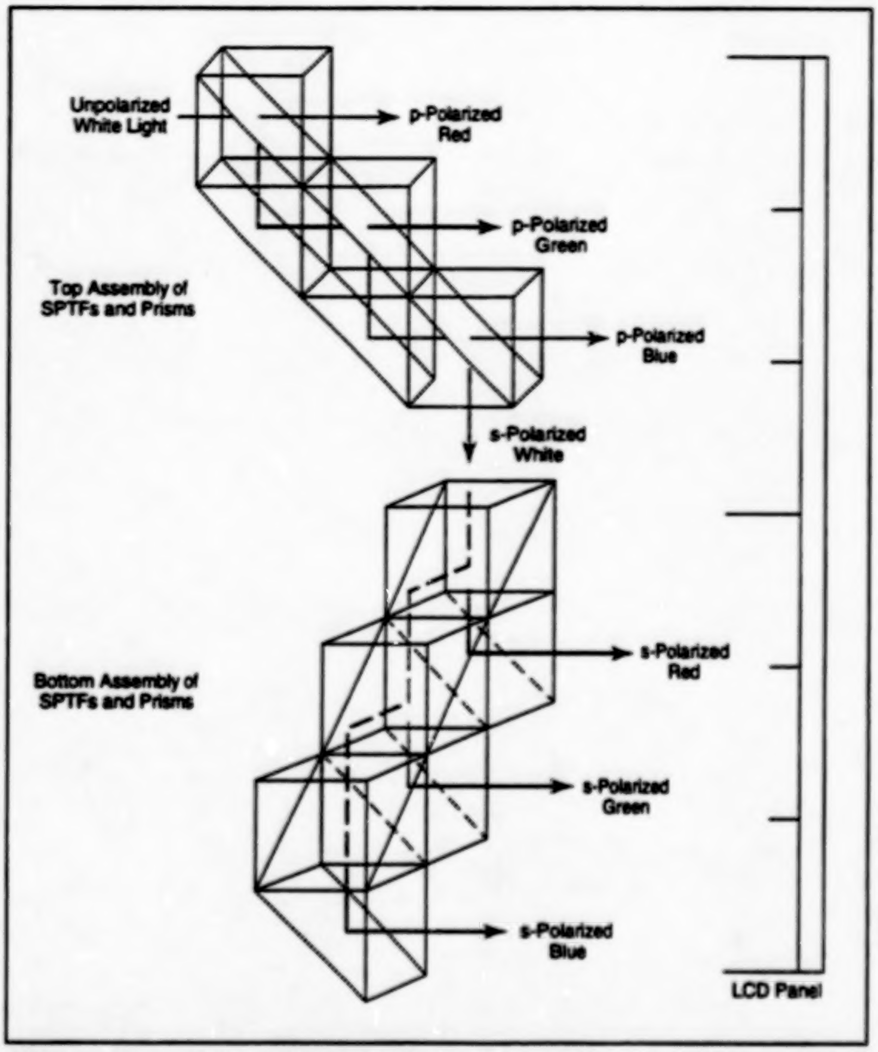

All Three Primary-Color and Both Polarization Components of the incident unpolarized white light would be utilized in this scheme. In contrast, a conventional color LCD device wastes about 5/6 of incident unpolarized light because it rejects one polarization component and two of the three color components.

to make the colors on the corresponding six subdivisions of the display area scroll downward or upward.

This work was done by Yu Wang of Caltech for **NASA's Jet Propulsion Laboratory**. *Further information is contained in a TSP [see page 1].*

In accordance with Public Law 96-517, the contractor has elected to retain title to this invention. Inquiries concerning rights for its commercial use should be addressed to

Technology Reporting Office
JPL
Mail Stop 122-116
4800 Oak Grove Drive
Pasadena, CA 91109
(818) 354-2240

Refer to NPO-20110, volume and number of this NASA Tech Briefs issue, and the page number.

Magnetic Random-Access Memories

Advantages include unlimited cyclability and radiation hardness.

NASA's Jet Propulsion Laboratory, Pasadena, California

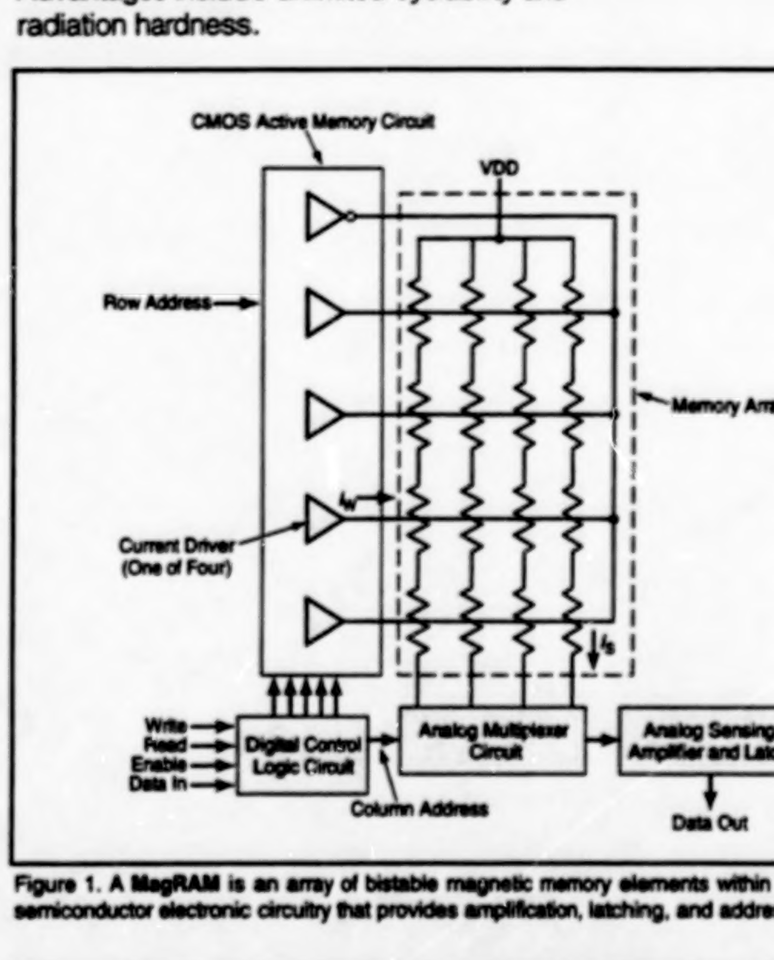

Figure 1. A MagRAM is an array of bistable magnetic memory elements within a matrix of semiconductor electronic circuitry that provides amplification, latching, and addressing.

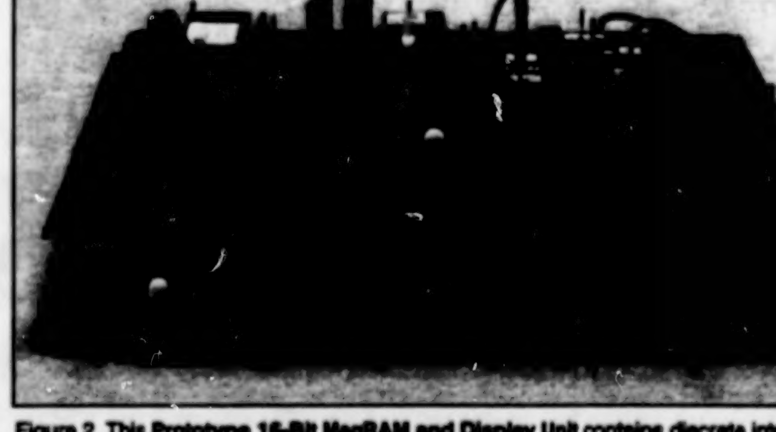

Figure 2. This Prototype 16-Bit MagRAM and Display Unit contains discrete integrated-circuit chips that would be combined into a single chip in an advanced production version.

A Magnetic Random-Access Memory (MagRAM) is an array of bistable magnetic memory elements with semiconductor amplifier and addressing circuitry. MagRAMs are in the early stages of development, which has been motivated by a need for nonvolatile memories with high densities and unlimited cyclability — a combination of properties that has not been achieved in nonvolatile electronic RAMs. In principle, the magnetic memory elements in MagRAMs can be made free of fatigue and thus capable of unlimited cyclability. Magnetic memory elements provide signals of reasonable magnitude that can be amplified by semiconductor electronic circuits, and offer the additional advantage of radiation hardness.

In a MagRAM, data is stored in the magnetic states of the magnetic memory elements, which are hysteretic. The data is read from these elements by using the magnetoresistive effect to sense their magnetization states. Figure 1 is a simplified schematic diagram of a 16-bit MagRAM. A designated bit element is addressed, for reading or writing, by the application of appropriate currents to the word-line (row) conductors and sensing-line (column) conductors that intersect at that element. The current in the word-line conductor generates the magnetic field to write a bit in the designated element. A bit (0 or 1) is written in an element by applying a sensing current I_S, together with a writing word current $-I_W$ for a 0 or $+I_W$ for 1. Nondestructive readout of the bit is effected by applying I_S with (a) a word current $-I_R$ followed by (b) a word current $+I_R$ (I_R<I_W). During readout, the analog sensing amplifier and latch act together to convert the change in voltage on the sensing line to a bit. The currents I_W, I_S, and I_R are chosen according to the hysteretic and magnetoresistive properties and the need to prevent spurious writing in inactive cells crossed by active word-line conductors.

A low-density 16-bit prototype MagRAM based on the concept is illustrated in Figure 2. This assembly is made from discrete

subsystems in the sense that the functional blocks indicated in Figure 1 are implemented by means of interconnecting separate integrated-circuit chips. Subsequent development efforts are expected to lead to the integration of all magnetic and electronic MagRAM components onto a single chip that would feature high memory density and low power consumption.

This work was done by Romney Katti and Brent Blaes of Caltech for **NASA's Jet Propulsion Laboratory**. *Further information is contained in a TSP [see page 1].*

In accordance with Public Law 96-517, the contractor has elected to retain title to this invention. Inquiries concerning rights for its commercial use should be addressed to

Technology Reporting Office
JPL
Mail Stop 122-116
4800 Oak Grove Drive
Pasadena, CA 91109
(818) 354-2240

Refer to NPO-20131, volume and number of this NASA Tech Briefs issue, and the page number.

Digital Approximation Premodulation Filter

This filter closely approximates the desired wave shape, regardless of the bit rate.

Dryden Flight Research Center, Edwards, California

A digital solution for the problem of filtering serial digital data prior to modulation of a telemetry transmitter has been developed by engineers at the Dryden Flight Research Center. The solution is described in a patent application entitled "DIGITAL APPROXIMATION PREMODULATION FILTER FOR PULSE-CODE-MODULATED SIGNALS."

When transmission of serial digital data for telemetry is required, care must be taken when modulating the transmitter to avoid any spurious radiated signals outside the assigned radio frequency band. A premodulation filter is used to eliminate undesired harmonics, thereby limiting the frequency bandwidth of the serial digital signal.

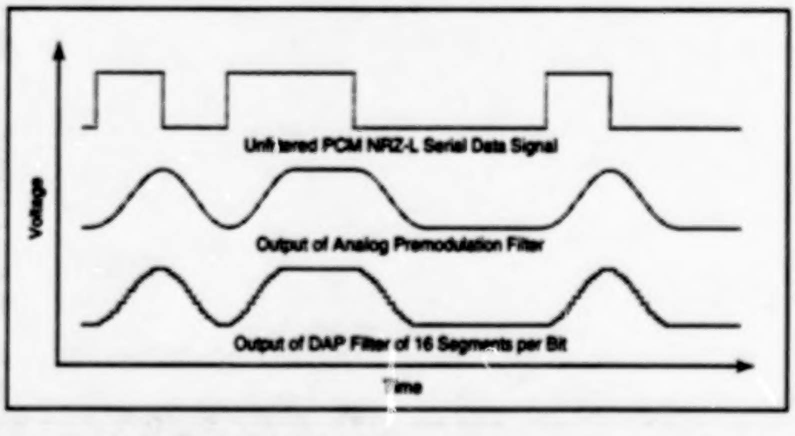

Figure 1. The **Digital Approximation Waveform** is a slightly degraded version of the output of an analog premodulation filter.

The use of a digital approximation (as distinguished from an analog) premodulation filter entails some degradation of the infinite output resolution of a traditional analog filter (see Figure 1), but this degradation should be tolerated in the interest of keeping out-of-band radiation below the maximum allowed by regulations.

The digital approximation premodulation (DAP) filter concept was tested in transmission of a pulse-code-modulation (PCM) system non-return-to-zero-level output via an L-band transmitter. Normally, 16 segments per bit are used, but in this test, the radiated frequency spectrum obtained when using the DAP filter with only 8 segments was essentially identical with that obtained when using an analog filter.

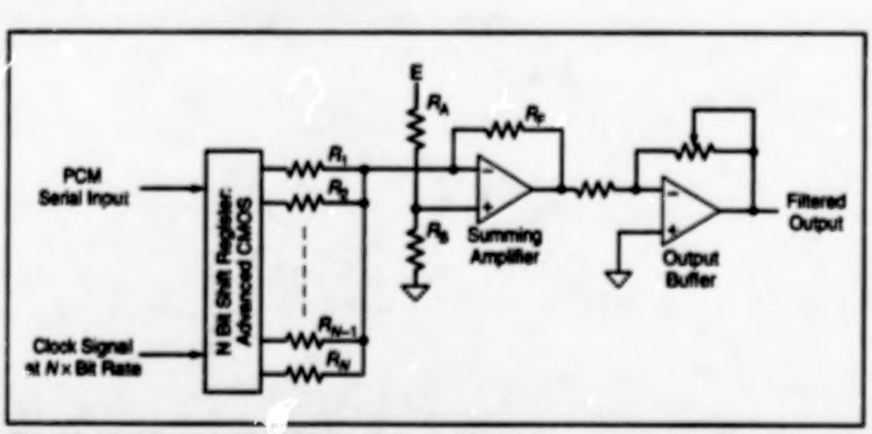

Figure 2. An ***N*-Segment DAP Filter** includes a shift register, a summing amplifier, and an output buffer.

The DAP filter (Figure 2) comprises three main parts: (1) a part that divides each bit into a number of segments, (2) a part that converts each segment into a voltage that approximates the output of an ideal premodulation filter, and (3) an output buffer amplifier. An integer frequency multiple of the bit-rate clock signal is used to shift the serial digital output through a parallel output shift register to segment each bit. The conversion to a voltage level can be accomplished by a resistor array and summing amplifier to approximate the rise or fall of a half cosine wave for each bit transition. If the integer frequency multiple of the bit-rate clock signal is not available from the signal source, it can be generated from the source bit-rate clock signal by use of a phase-lock loop.

Because the DAP filter is synchronized with the bit-rate clock as described above, it always produces the proper wave shape, regardless of the bit rate of the unfiltered data signal.

This work was done by Harry Chiles and Rod Bogue of **Dryden Flight Research Center**.

This invention is owned by NASA, and a patent application has been filed. Inquiries concerning nonexclusive or exclusive license for its commercial development should be addressed to the Technical Information Specialist, Dryden Flight Research Center, (805)258-3720. Refer to DRC-95-28.

Surface-Plasmon Reflective Flat-Panel Color Displays

These displays would be readable in ambient light.

NASA's Jet Propulsion Laboratory, Pasadena, California

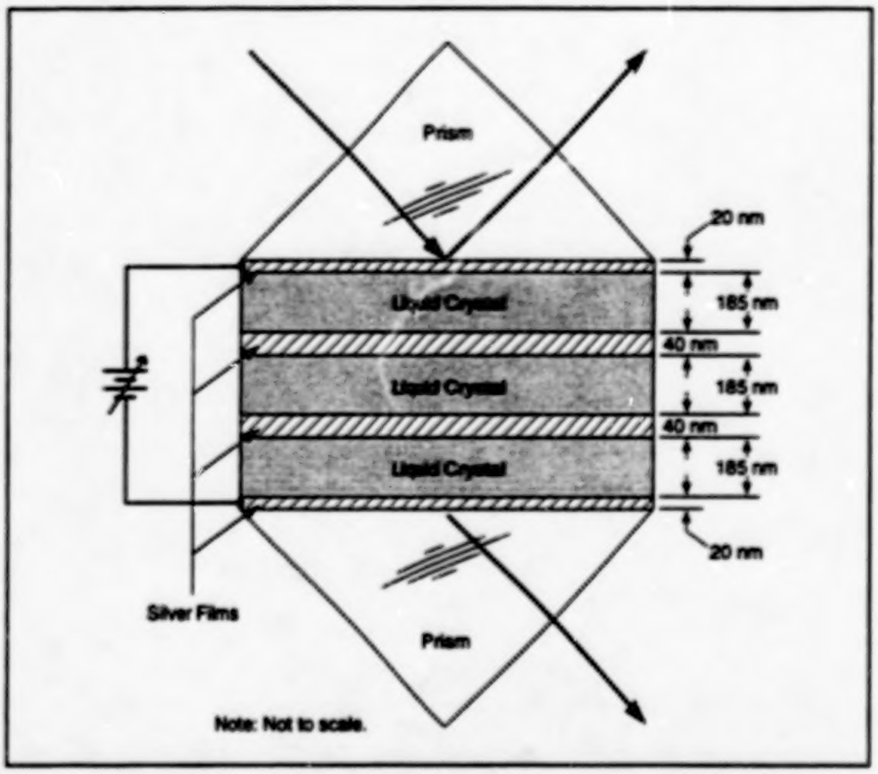

Figure 1. A Surface-Plasmon Optoelectronic Device of this general configuration would exhibit the desired voltage-tunable notch-filter characteristic, according to theoretical calculations.

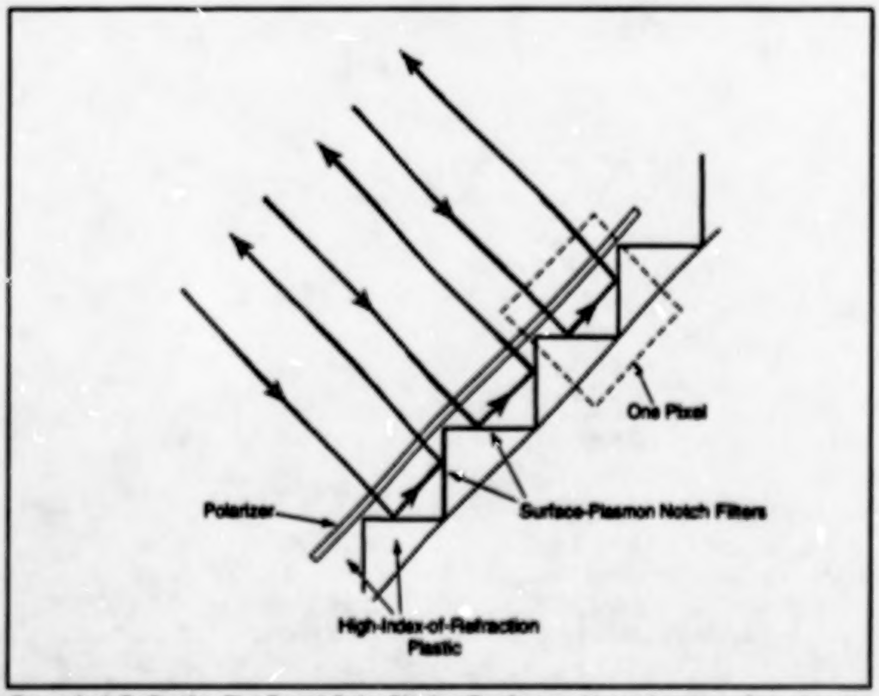

Figure 2. A Reflective Flat-Panel Color Display Device would contain two surface-plasmon notch filters, similar to that shown in Figure 1, in each pixel.

Reflective flat-panel color display devices based on surface plasmons are undergoing development. Heretofore, no reflective flat-panel color display devices have been available. The active matrix liquid-crystal devices now used to provide flat-panel color displays must be lit internally, are power-hungry (typically consuming about 80 percent of the power of a laptop computer), and cannot be read in bright ambient light. In contrast, the surface-plasmon display devices would be operated without internal lighting, would consume much less power, and would be readable in bright ambient light (including sunlight).

This development is based on voltage-induced color-selective absorption of light in surface plasmons: When a surface-plasmon wave is excited at a metal/liquid-crystal interface, the absorption spectrum of surface-plasmon resonance can be shifted across the visible range by altering a voltage applied to the liquid crystal. This effect can be exploited to make a tunable notch filter — more specifically, a filter that absorbs most of the incident light in a voltage-adjustable wavelength range (the "notch") and reflects most of the incident light outside that range. If incident white light can be reflected from two tunable notch filters in succession and if the absorption wavelength range of each filter can be made to span about 2/3 of the visible spectrum, then by suitable choice of the notch wavelengths, the resulting display can be made to appear black (most of the incident light absorbed), white (most of the incident light reflected), or any primary color at a selectable level of brightness.

The problem then becomes one of how to implement a voltage-tunable notch filter and to combine a number of such filters into an array of pixels to construct a flat-panel display device. Figure 1 illustrates such a filter, which includes two high-index-of-refraction prisms for coupling, plus four silver films interspersed with three liquid-crystal layers. Surface-plasmon waves are excited at the six liquid-crystal/metal-film interfaces, and the layers are made sufficiently thin that the surface-plasmon waves are coupled together. When a voltage is applied between the two outermost silver films, the device acts electrically like three capacitors in series, and the electric field affects the indices of refraction of the liquid-crystal layers, causing a wavelength shift of the absorption spectrum. A theoretical calculation shows that this filter would exhibit the desired notch characteristic, that with no voltage applied, it would absorb primarily in blue-green light, and that its absorption

wavelength region could be shifted to red or beyond by applying increasing voltage.

Figure 2 shows part of a proposed flat-panel display device, wherein each pixel would contain two notch filters. The prisms — now microscopic to fit the pixels — would be molded into sheets of high-index-of-refraction plastic. A polarizer sheet would be mounted on the front surface to select p-polarized light. After polarization, the incident light would be reflected from one notch filter, then from the other notch filter. By choice of the voltages applied to the two notch filters in each pixel, one could obtain a desired color combination as described above.

This work was done by Yu Wang of Caltech for **NASA's Jet Propulsion Laboratory**. *Further information is contained in a TSP [see page 1].*

In accordance with Public Law 96-517, the contractor has elected to retain title to this invention. Inquiries concerning rights for its commercial use should be addressed to

Technology Reporting Office
JPL
Mail Stop 122-116
4800 Oak Grove Drive
Pasadena, CA 91109
(818) 354-2240

Refer to NPO-20244, volume and number of this NASA Tech Briefs issue, and the page number.

Prolonging the Lives of Rechargeable Lithium-Ion Cells

Proposed modifications would prevent dissolution of metal current collectors.

NASA's Jet Propulsion Laboratory, Pasadena, California

Several modifications of the design and operation of lithium-ion rechargeable electrochemical cells have been proposed to prolong the cycle lives of the cells. As explained below, overdischarge can result in dissolution of a metal current collector in the anode of a cell, with consequent internal short-circuiting of the cell and thus loss of cycle life. The proposed modifications are intended to prevent dissolution of the metal current collector and thereby extend the cycle life.

In a typical cell of the type in question, the active cathode material is a lithiated oxide (e.g., Li_xCoO_2) and the active anode material is carbon. These active materials are coated on different substrates or current collectors to make electrodes, and separator paper is used to prevent contact between the two electrodes. The current-collector materials must be chosen for compatibility with the cell chemistry; for example, the anode current collector can be made of copper or nickel.

A freshly fabricated cell is fully discharged: All the lithium is stored in the lithiated oxide cathode material; there is no lithium in the carbon anode material. An initial charging process is necessary to activate the cell. During the charging process, lithium becomes deintercalated from the Li_xCoO_2 cathode material and intercalated into the carbon anode material; the reverse happens when the cell is discharged.

In this context, overdischarge of a previously charged cell can be defined as continuation of discharge after all the reversible lithium has been completely depleted from the carbon anode material. Initial charging of a freshly fabricated cell in reverse polarity is equivalent to overdischarging a previously discharged cell. The figure shows the relative potentials (vs. Li) for relevant materials in a lithium-ion cell with a copper current collector in the anode. During overdischarge or reversal of polarity, the potential of the graphite anode rises above the potential of the copper current collector, causing the formation of a spurious cell between Li_xCoO_2 and copper. The copper then begins to dissolve, causing a short circuit.

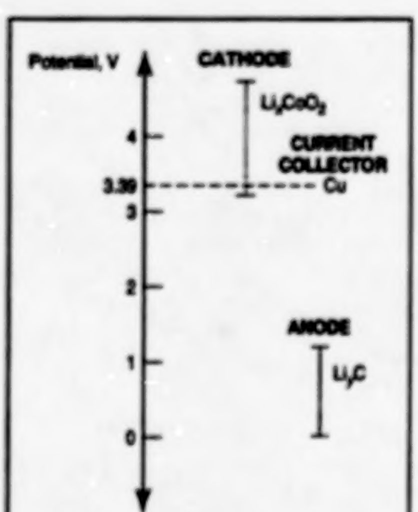

The Potentials (Relative to Lithium) of cathode, anode, and current-collector materials affect the charge, discharge, and overdischarge behavior of a lithium-ion cell.

The following are the proposed modifications for preventing dissolution of the anode current collector:

1. Raise the cell potential below which discharge is cut off ("discharge cutoff voltage," for short). For example, in a graphite/Li_xCoO_2 Li-ion cell with a cathode/anode weight ratio of 3, the cycling voltage range is between 4.1 V (charge cutoff) and 3.0 V (discharge cutoff). If the discharge cutoff voltage were raised to 3.5 V, the consequent loss of capacity would be only 10 mA·h, while the cycle life would be extended.
2. Configure both internal and external electrical connectors to prevent reversal of polarity in a freshly fabricated cell, and verify correct polarity of connections to test equipment before conducting a test.
3. Use cathode additive(s) for protection against overdischarge, as described in "Preventing Overcharge and Overdischarge of Lithium Cells" (NPO-18343), NASA Tech Briefs, Vol. 19, No. 3 (March 1995), page 36. Low-potential cathode additives could help to reverse the potential of the spurious cell so that the copper current collector would not dissolve.
4. Make the anode current collector out of carbon instead of copper. This could be done, for example, by coating a carbon-based material onto an electrically conductive polymer or onto a sheet of separator paper to make an anode.

This work was done by Chen-Kuo Huang of Caltech for **NASA's Jet Propulsion Laboratory**. *Further information is contained in a TSP [see page 1].*

In accordance with Public Law 96-517, the contractor has elected to retain title to this invention. Inquiries concerning rights for its commercial use should be addressed to

Technology Reporting Office
JPL
Mail Stop 122-116
4800 Oak Grove Drive
Pasadena, CA 91109
(818) 354-2240

Refer to NPO-19897, volume and number of this NASA Tech Briefs issue, and the page number.

Optical Power Supply and Data Communication for APS Circuits

There would be no electrical connections with external circuits.

NASA's Jet Propulsion Laboratory, Pasadena, California

Active-pixel-sensor (APS) circuits and perhaps other dense complementary metal oxide/semiconductor (CMOS) very-large-scale integrated (VLSI) circuits would be powered by infrared beams transmitted by laser diodes and received by photodetectors, according to a proposal. Clock signals for synchronizing the operations of such a circuit would be transmitted as modulation on the infrared power-supply beam. Command data signals could be received via other low-power infrared beams. Digital APS output signals would likewise be sent to external circuits via modulation of infrared beams transmitted by low-power laser diodes incorporated into the VLSI APS chips.

The power-supply part of the proposal has been made feasible by advances that have reduced the power demands of CMOS VLSI circuits. The power demand of a typical CMOS VLSI APS chip is now low enough that a single, sufficiently illuminated infrared photodetector could serve as the source of a galvanically isolated power supply on the chip. With a sufficiently high duty factor, the clock modulation on the infrared power-supply beam should exert little effect on power-coupling efficiency.

The data-communication part of the proposal has been made feasible by the evolution of sensitive infrared detectors and low-power, frequency tunable laser diodes. The infrared beams for input and output of data would have wavelengths different from that of the power-input beam. By use of tuned laser diodes in the transmitters and narrow-band dielectric filters in the receivers, it would be possible to communicate simultaneously over multiple infrared bands; thus, it would be possible to use a wavelength-multiplexing scheme to achieve a high data rate.

Multiple CMOS VLSI APS chips could be operated under common control and readout by use of a combination of wavelength and time multiplexing. The multiplexing scheme could be simplified, at the cost of some increase in structural complexity, by using a dedicated optical fiber for data communication between each APS and the common readout and control circuitry.

As APS and other VLSI circuits become denser and more complex, design problems pertaining to reliability of, and power dissipation in, electrical interconnections, become increasingly difficult. The problems are further intensified in cases in which VLSI circuits are required to be connected together in many-to-one networks. In general, the complexity of, and power dissipation in, electrical interconnections increase approximately exponentially with the number of nodes, while reliability decreases approximately exponentially with the number of nodes. The use of all-optical input and output connections according to the proposal described above could reduce overall complexity and increase reliability. In particular, if full-duplex communication with frequency multiplexing of data signals were used, then the complexity of a network with all optical interconnections would increase only linearly with the number of nodes.

This work was done by Frank Hartley and Bedabrata Pain of Caltech for **NASA's Jet Propulsion Laboratory**. *Further information is contained in a TSP [see page 1].*
NPO-20438

GaAs-Membrane-Diode Mixer for Operation at 2.5 THz

The design is readily scalable to other frequencies.

NASA's Jet Propulsion Laboratory, Pasadena, California

A prototype mixer designed for operation at input frequencies near 2.5 THz incorporates a planar Schottky-barrier diode and a radio-frequency (RF) filter that are parts of an integrated circuit on a GaAs membrane strip, plus several other unique features for which there are numerous potential applications. This mixer is intended to provide a less expensive, more reliable alternative to older whisker-contact-diode mixers. The components of the mixer are integrated into a robust package with an overall volume <1 in.^{3} (<16 cm^3). The design can readily be scaled to higher and lower frequencies.

The GaAs structure is monolithic and is patterned to form circuit elements by use of photolithographic techniques. The GaAs structure includes the membrane strip suspended over a rectangular hole in a rectangular frame (see Figure 1). The membrane strip serves as part of a low-loss transmission line and RF-coupling structure as well as a support and as an integral part of the diode and other circuit

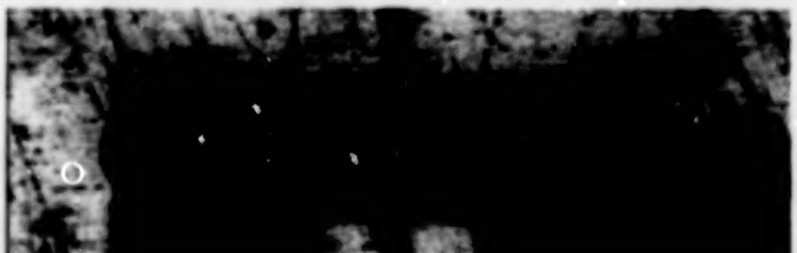

Figure 1. Integrated Circuitry is formed on top of the monolithic GaAs structure. The planar Schottky diode, shown at the highest magnification, includes an air-bridge contact finger and stress-relief air bridges at both ends.

elements. The strip is 3 µm thick by 40 µm wide by 600 µm long; other dimensions could be chosen according to the intended operating frequency and requirement for mechanical rigidity. Beam leads for electrical contact with external circuitry are formed on the GaAs structure.

The GaAs structure is glued into a copper button with a diameter of 0.175 in. (4.4 mm) and a thickness of 0.075 in. (1.9 mm). The button contains a 2.5-THz rectangular waveguide, a rectangular-to-circular waveguide transition, and an integrated dual-mode conical feed horn (see Figure 2.) The copper button is fabricated by electroforming plus conventional machining. The desired alignment of the GaAs structure with respect to other circuit elements is enforced by use of a reference surface milled into the button. The button is pressed into a larger block (see Figure 2), made of brass, that holds a fixed (but replaceable) waveguide tuner section containing a backshort, a separate intermediate-frequency (IF) quartz suspended stripline impedance transformer, and a coaxial connector to couple with such external circuitry as an IF amplifier or a splitter.

In operation, the local oscillator and the RF signal of interest enter the mixer via the feed horn. The input signals are combined at the diode and the beat-frequency output signal (that is, the IF signal) is removed via the RF filter on the membrane, the quartz impedance transformer, and the coaxial connector. There is no tuning during operation except what can be achieved by adjustment of the dc bias on the diode. The optimal backshort setting is determined in a trial-and-error procedure in which the mixer is operated with tuner sections of various waveguide lengths inserted in the block.

Figure 2. The Mixer Is Packaged in two half blocks of brass. Shown here is the lower half block containing the button and the transformer.

This work was done by Peter H. Siegel, R. Peter Smith, Suzanne Martin, Peter Bruneau, and Michael Gaidis of Caltech for **NASA's Jet Propulsion Laboratory**. *Further information is contained in a TSP [see page 1].*

In accordance with Public Law 96-517, the contractor has elected to retain title to this invention. Inquiries concerning rights for its commercial use should be addressed to

Technology Reporting Office
JPL
Mail Stop 122-116
4800 Oak Grove Drive
Pasadena, CA 91109
(818) 354-2240

Refer to NPO-20397, volume and number of this NASA Tech Briefs issue, and the page number.

Three-Level Buck dc-to-dc Converter for Low Temperature

This circuit is fully functional at temperatures from room down to liquid-nitrogen temperature.

Lewis Research Center, Cleveland, Ohio

A dc-to-dc switching power converter of the three-level, pulse-width-modulated, buck type has been designed, built, and verified to operate at temperatures from ambient down to −196 °C (the temperature of liquid nitrogen). Circuits like this one could be useful for supplying electric power to low-temperature circuits in such diverse applications as cryogenic instruments, superconductive magnetic energy-storage systems, magnetic-resonance imaging systems, high-speed computer and communication systems, and high-power motor and generator systems.

The design of a multilevel switching dc-to-dc power converter exploits series connection of power semiconductor switches. The sharing of voltage among the series-connected switches, especially during turn-on and turn-off transients, is a major design issue. The duty factor (switch "on" time to duration of switching cycle) can be chosen to obtain a desired input-to-output voltage ratio. Also, different switches can be turned on and off at different times (equivalently, the switches can be operated at different phase shifts rela-

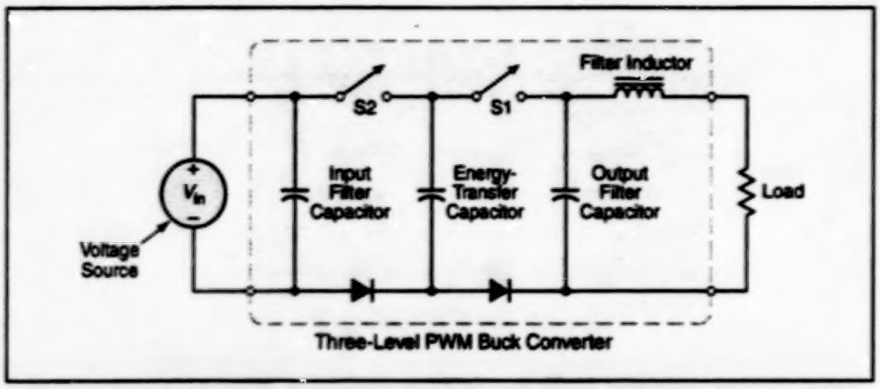

A Three-Level, Pulse-Width-Modulated, Buck-Type dc-to-dc Converter offers an advantage over a two-level converter of the same type; namely, that the voltage stresses on the semiconductor components are lower.

tive to each other and to the overall switching cycle) to minimize the generation of harmonics in the filtered output of the converter.

A three-level converter of the present type (see figure) is a special case of a multilevel switching buck dc-to-dc power converter. In comparison with a standard two-level converter, the three-level converter contains one more switch, one more diode, and one more capacitor. An n-level converter (where $n > 2$) offers an advantage over a standard two-level converter; namely, that the voltage ratings applied to the semiconductor devices in the n-level converter are decreased to $1/(n-1)$ of those of the two-level converter; the reduction in voltage stresses on semiconductor switches and diodes effects a reduction in switching and conduction losses, and enables the use of semiconductor components with correspondingly lower voltage ratings.

The present three-level converter was designed and constructed using standard, commercially available components, including power metal oxide/semiconductor field-effect transistors (MOSFETs), ultrafast semiconductor power rectifiers, complementary metal oxide/semiconductor integrated circuits for pulse-width modulation and control, metallized-polypropylene-film energy-transfer and output capacitors, and an inductor with a core made of a high-permeability powder. The requirement for low-temperature operation was taken into account in the selection of all components. The design specifications include an input potential of 48±10 V; an output potential of 12 V; an output voltage ripple of 120 mV (1 percent of rated output voltage); minimum and maximum load currents of 1 and 5 A, respectively; maximum output power of 60 W, and a switching frequency of 50 kHz.

The converter was tested in operation at temperatures from 25 down to −195 °C. At room temperature, the converter operated with an efficiency of 89.12 percent. At −195 °C, the measured efficiency was slightly lower; namely, 87.27 percent. Even at −195 °C, the converter was found to be fully functional.

This work was done by Richard L. Patterson of **Lewis Research Center** *and Fausto F. Pérez-Guerrero and Biswajit Ray of the University of Puerto Rico. Further information is contained in a TSP* [*see page 1*].

Inquiries concerning rights for the commercial use of this invention should be addressed to NASA Lewis Research Center, Commercial Technology Office, Attn: Tech Brief Patent Status, Mail Stop 7-3, 21000 Brookpark Road, Cleveland, Ohio 44135. Refer to LEW-16675.

Novel Full-Color Cathode Ray Tube for Miniature-Display Applications

Piezoelectric-actuator-controlled, movable-screen, single-electron-gun design enables miniaturization of high-resolution, high-brightness, full-color CRTs for small-display applications.

NASA Lewis Research Center, Cleveland, Ohio

A novel cathode ray tube (CRT), using a single electron gun and a movable screen, has been developed that now enables miniaturization of a full-color CRT with the same excellent viewing quality customarily found in larger-screen CRTs. In addition to the benefits of wide viewing angle, high resolution, high brightness, color purity, and full gray-scale features that are characteristic of CRTs, the need for only one electron gun is expected to also result in reduced power consumption and lower cost. The movable-screen design, a significant improvement over the earlier moving-shadow-mask version (1), is considered feasible for CRTs ranging in size from less than 1 in. (2.5 cm) to greater than 5 in. (12.7 cm). A unique and highly advantageous feature of the improved design, which is described in greater detail below, is the elimination of spatial offset of the color pixels. One obvious application with great commercial potential is in helmet-or head-mounted displays for a wide variety of virtual-reality systems. Other applications include portable or hand-held devices where compactness, low power, high resolution, and high brightness are desirable or advantageous, such as TVs, monitors for VCRs, and viewfinders for camcorders, especially for outdoor use.

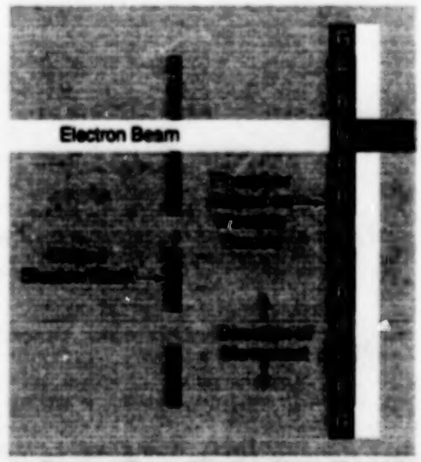

An Electron-Beam Shadow-Mask Movable Screen Region is illustrated in this top view.

The conventional CRT uses three electron guns, one for each primary color (red, green, blue), plus a stationary slotted or otherwise perforated shadow mask aligned with the color phosphors on the glass screen. The geometrical relationship between the mask and the guns is designed so that the electron beam from each gun impinges on only the phosphor dots of the desired primary color. Accurate alignment of the guns, shadow masks, and phosphors is critical to the purity of the primary colors and resolution of the display. Achieving the beam convergence

and registration required for high resolution becomes extremely difficult for a miniature full-color CRT with three electron guns and is, therefore, commercially impracticable. Other single-electron-gun designs, such as the beam index tube and color shutter tube, lack either the high resolution or high brightness desirable for most miniature-display applications. By default, the miniature color display market is presently dominated by flat-panel displays (FPDs), the most common of which is the active matrix liquid crystal display (AMLCD). This and all other miniature FPDs, either presently on the market or under development, have one or more of the following drawbacks: poor resolution (graininess), low brightness, narrow viewing angle, high cost, or high power consumption. The miniature full-color CRT described here has none of these drawbacks.

A simplified representation of the electron beam — slotted shadow mask — movable screen region is shown in the figure. In contrast to the earlier version (1), the shadow mask remains stationary and the moving part is a thin inner glass sheet that contains the parallel red-green-blue phosphor stripes and is mounted on piezoelectric actuators for precisely controlled movement. To write a given primary color, the electron gun is activated at the beam intensity needed to obtain the desired brightness. At the same time, the piezoelectric actuators are energized to align the phosphor stripes of that color with the slots in the shadow mask and also mask the other two colors with the solid portion. The entire color field is written before the screen is moved to uncover the next color. Full color is achieved by overlaying the three-color fields in time. In the improved movable screen version, the moving element is much lighter; thus shortening the hold-off time between color changes to less than 140 ms. If the mask is not perfectly aligned with the phosphor stripes during assembly of the CRT, it can be accomplished electronically during monitor calibration by applying dc-offset voltages to the piezoelectric actuators. The capability for electronic alignment is an important feature that offers not only the possibility of greater color purity and brightness, but also lower manufacturing cost by reducing the elaborate jigging required for alignment during assembly of the conventional shadow mask CRT. Having the light-emitting element—the screen—moving is a great advantage because the color pixels have no spatial offset as seen by the viewer. Up close, the viewer sees one composite color dot, not three primary color dots that the eye must then attempt to integrate. Except for the color shutter tube, which is seriously lacking in brightness, this feature is not found on other displays including conventional CRT's, AMLCDs, and FEDs (fuel-emission displays). It is particularly important where close-in viewing is necessary, such as in helmet-mounted displays.

A further improvement contributing to lower cost is assembly of the mask and actuator components on a laser-cut, multilayer ceramic stack with printed-circuit elements to power the piezoelectric actuators. The ceramic stack is part of the vacuum envelope wall and leads to lower part count, less complexity, and better alignment and rigidity.

By providing the means to rapidly move objects in vacuum with amplitudes up to 0.015 in. (0.38 mm) also the capability to withstand temperatures up to 450 °C, this work advances the state of piezoelectric technology. It is expected to find application in other areas, such as sensors and MEM (micro electromechanical) devices.

(1) B.K. Vancil and E.G. Wintucky, *Ultrahigh Resolution Miniature Color CRT for Virtual-Reality Applications*, Proceedings of 5th National Technology Transfer Conference (Technology 2004), Vol. 2, NASA Conference Publication 3313, 1994.

This work was done by Bernard K. Vancil of FDE Associates for **Lewis Research Center.** *Further information is contained in a TSP [see page 1].*

Inquiries concerning rights for the commercial use of this invention should be addressed to NASA Lewis Research Center, Commercial Technology Office, Attn: Tech Brief Patent Status, Mail Stop 7–3, 21000 Brookpark Road, Cleveland, Ohio 44135. Refer to LEW-16187.

BLANK PAGE

16

Electronic Systems

Hardware, Techniques, and Processes

BLANK PAGE

18

Partitioned Frequency-Division Multiplex for Bandwidth Compression

Spectrum would be utilized more efficiently than in CDMA and FDMA.

NASA's Jet Propulsion Laboratory, Pasadena, California

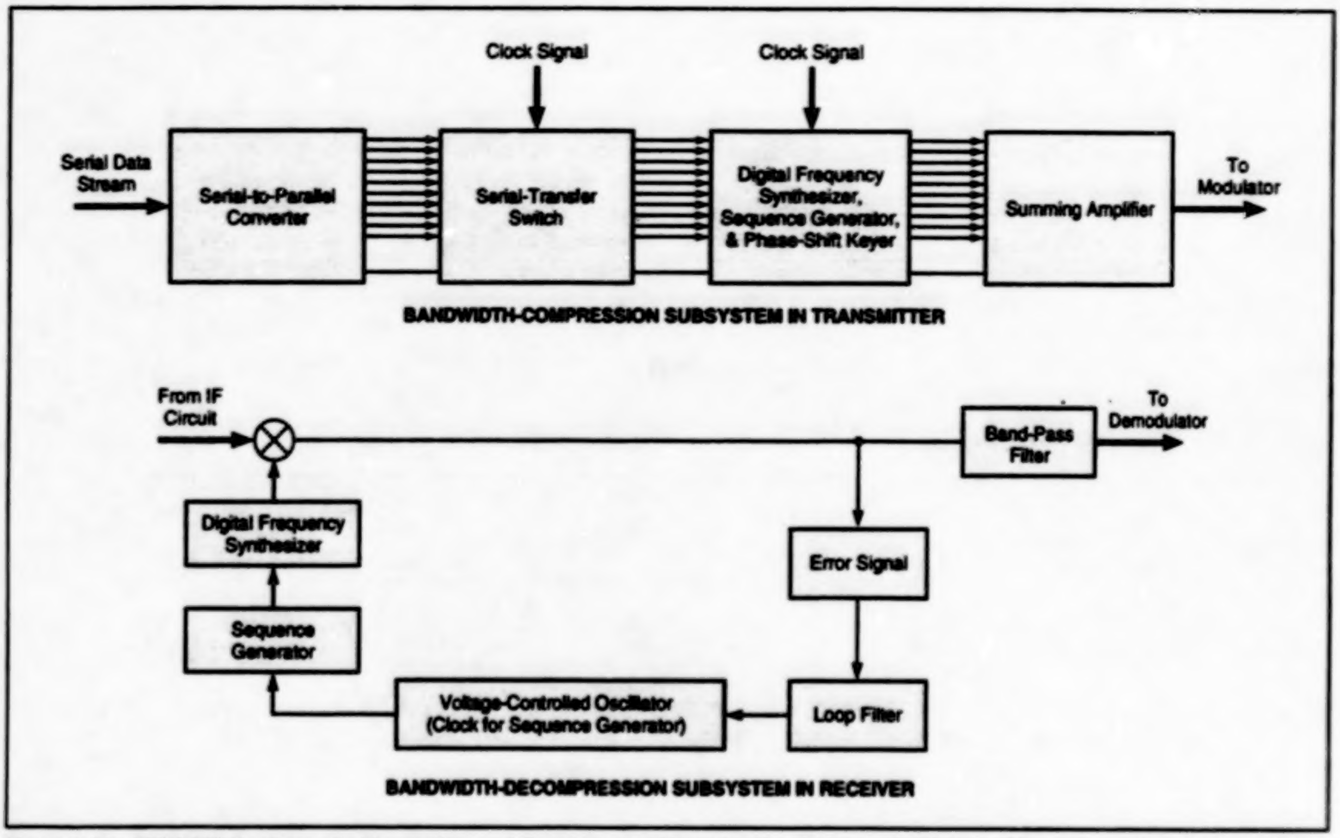

Figure 1. The **FH/PFDM Portions of a Transmitter and Receiver** would increase the efficiency of utilization of the radio spectrum for transmitting a data stream of a given rate.

Frequency-hopped and partitioned frequency-division multiplex (FH/PFDM) is a proposed modulation technique for transmission of digital signals. In FH/PFDM, a serial stream of data (possibly generated by multiple users) coming into a transmitter would be distributed into frequency-hopped, frequency-partitioned subchannels, in such a way as to reduce (in comparison with other modulation techniques) the overall carrier deviation and sidelobe excursion.

Figure 1 presents block diagrams of the bandwidth-compression and -decompression portions of an FH/PFDM transmitter and receiver, respectively. In the transmitter, the incoming data stream to be transmitted would first be converted from serial to parallel format and grouped into data blocks of n slots, each slot corresponding to one of n subcarrier frequencies generated by a digital frequency synthesizer. Next, a serial transfer switch would transfer the data bits into a buffer. Under sequential strobing by clock pulses, data bits would be strobed from the buffer into modulo-2 adders, the outputs of which would be modulated onto the subcarriers by phase-shift keying (PSK). The data bits would be interleaved in the sense that each successive data bit would be phase-modulated onto one of the subcarriers in a sequence of increasing subcarrier frequencies.

Meanwhile, under synchronization by clock pulses from a sequence generator, the frequencies of the n subcarriers would periodically be made to hop; during each clock cycle of the sequence generator, each subcarrier would hop through a total of m different frequencies (see Figure 2).

n Subcarriers

m Hops

	$i = 1$	$i = 2$	.....	$i = 10$
$j = 1$	202	212	.....	292
$j = 2$	203	213	.....	293
⋮	⋮	⋮	Frequencies are in kilohertz.	⋮
$j = 1$	211	221	.....	301

Figure 2. **This Table Lists Subcarrier Frequencies** for an example of an array of $n = 10$ subcarriers and $m = 10$ hops. Each cell (i,j) in the table gives the frequency of the ith subcarrier during the jth interval between frequency hops.

The purpose of the hopping is to achieve spectral isolation between subchannels and thereby reduce self-interference. Finally, the PSK subcarriers would be combined in a summing amplifier, which, in turn, would be used to modulate a carrier signal by frequency-shift keying (FSK).

In the receiver, a digital frequency synthesizer driven by a sequence generator would produce the same array of *n* frequencies and sequence of *m* frequency hops as that of the transmitter. This array of hopped frequencies would serve as a local-oscillator signal for use in asynchronously demodulating the received modulated subcarriers. The local-oscillator signal would be multiplied by the incoming intermediate-frequency (IF) signal in a mixer. An error signal derived from the mixer output would be used to control the sequence-generator clock frequency. The mixer output would also be band-pass filtered to remove unwanted mixer products, then passed on to a demodulator.

Theoretical calculations have shown that FH/PFDM would make it possible to utilize the available spectrum more efficiently than is possible in the established techniques of code-division multiple access (CDMA) and frequency-division multiple access (FDMA). In other words, for a given equivalent communication-link power, and performance, FH/PFDM would accommodate a greater number of users or a greater overall data rate in a given bandwidth or, equivalently, require less bandwidth for a given overall data rate or number of users. The cost of this spectrum compression would be an increase in the complexity of transmitters and receivers. One potential additional advantage FH/PFDM is that by interleaving the data and ordering the frequency hops in pseudorandom sequences, one could help to prevent unauthorized interception of data. The most practical route to realization of the potential of FH/PFDM would likely be to develop application-specific integrated circuits to implement the FH/PFDM transmitting and receiving functions.

This work was done by Charles Ruggier of Caltech for **NASA's Jet Propulsion Laboratory**. *Further information is contained in a TSP [see page 1].*
NPO-20364

Desktop Computer System Processes Satellite Data

This system is reconfigurable, easy to use, compact, and relatively inexpensive.

Goddard Space Flight Center, Greenbelt, Maryland

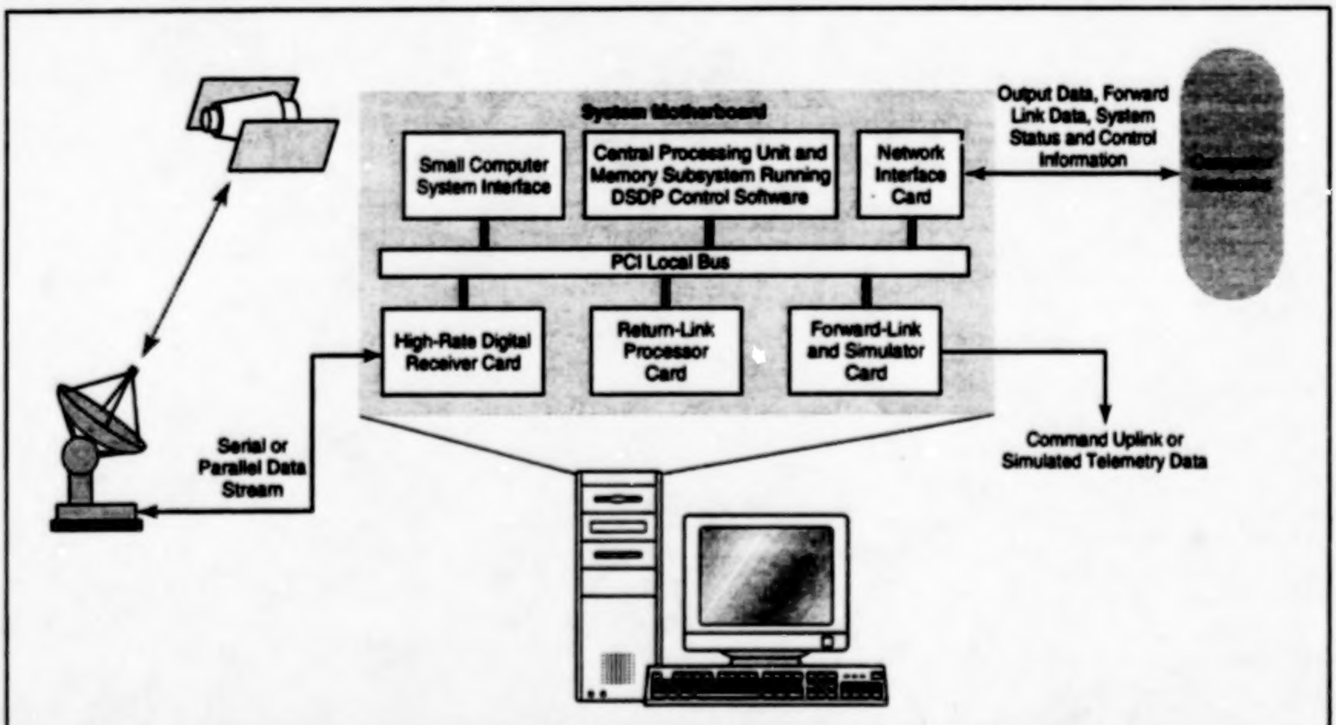

The DSDP Acts as an Earth/Satellite Gateway that communicates with other terrestrial computer systems (from which commands are received and to which telemetry data are delivered) via standard commercial computer-network interfaces.

The Desktop Satellite Data Processor (DSDP) is a prototype computer system for processing telemetry data received from, and command data to be transmitted to, a spacecraft in orbit around the Earth (see figure). The design of the system utilizes very-large-scale integrated (VLSI) application-specific integrated circuits (ASICs), parallel computer architectures, and pipelined data processing. Advanced software and a high level of integration of hardware and software components are expected to make a fully developed version of the system fit into a desktop-sized package at relatively low cost; the fully developed system is expected to be less than one-fourth as large as an equally capable system made entirely from commercial off-the-shelf (COTS) components.

The DSDP contains ASIC components that perform frame synchronization, Reed-Solomon decoding, and other standard telemetric processing functions (e.g., sorting and annotation of data packets) that are denoted generally as "service processing" and are performed according to recommendations of the Consultative Committee for Space Data Systems (CCSDS). The ASIC components are integrated onto cus-

tom-designed, highly reusable circuit cards based on the industry-standard peripheral component interconnect (PCI) bus. By high-level integration of the telemetry-processing functions into VLSI chips and cards, the design of the system affords high performance and high reliability and, relative to older telemetry systems, low cost.

The DSDP hardware comprises several custom-designed PCI-bus modules containing the ASIC circuit cards plus COTS components. The functions of the modules, ASICs, and COTS components are integrated by use of the DSDP control software, which provides a generic environment for controlling and monitoring diverse hardware components within a system.

The DSDP control software is a distributed, modular, platform- (operating-system)-independent, highly reconfigurable, reusable, software system that facilitates customization by and for users and is easily modifiable to support system upgrades and new system components. It affords a general-purpose capability for displaying data and creating graphical user interfaces for controlling and monitoring systems. The graphical user interfaces are easy to use (and highly automated) making it possible for a nonspecialist to configure and operate the system. The software also includes tools for planning and scheduling operations, and for the management, processing, generation, and assurance of the quality of, scientific data products. These characteristics make the DSDP control software attractive for other applications that involve scheduling, planning, and the distribution of data; examples include medical, banking, stock-exchange, and automotive-production applications.

This work was done by Barbie Brown, Parminder Ghuman, Jeremey Jones, Johnny Medina, and Greg Schmidt of **Goddard Space Flight Center**; *Tom Brooks, Lisa Koons, and Randy Wilke of Century Computing Inc.; John Stachniewiczs and Keith Wichmann of GS&T; and Daryl Halliday of Visix. Further information is contained in a TSP [see page 1].*
GSC-14036

Snapshot CCD Camera With Microelectromechanical Shutter

Microscopic actuated mirrors would divert light from the CCD at selected times.

NASA's Jet Propulsion Laboratory, Pasadena, California

A proposed charge-coupled-device (CCD) camera would be mechanically shuttered by a planar array of micromachined, electromechanically actuated shutters. This proposal has arisen as part of the solution to the problem of designing a visible/near-infrared imaging spectrometer using a commercial off-the shelf CCD as the image sensor at the focal plane. The need for mechanical shuttering arises because the desired exposure time clashes with the readout times of available CCDs. In particular, what is needed is an exposure time shorter than the readout time. By use of the array of micromachined mirrors, the image could be deflected off the focal plane during the readout cycle to prevent contamination of the captured image with light after the desired charge-integration (exposure) time.

According to the proposal, an object would be imaged on the focal plane via a folding mirror. In this case, the folding mirror would be the array of micromachined mirrors. Such arrays have been fabricated before for other purposes and are examples of what are now denoted generically as microelectromechanical systems (MEMS).

The elements of the array would be of the order of 10 by 10 μm. The mirrors would be operated in a binary mode, in which they would be switched between extreme angular positions 10° apart at megahertz rates. In the normal or unactuated state (mirrors at one of the extreme angular positions), the mirrors would reflect the image light onto the focal plane. In the fully actuated state (mirrors at the other extreme angular position), the mirrors would deflect the image light away from the focal plane and onto a beam dump, which would absorb the light. The exposure time could be set by setting the duty cycle of the two mirror states.

Unlike traditional iris- and leaf-type mechanical shutters, the proposed MEMS-type shutter would be capable of closing off the entire image at once, and would operate without appreciable jitter. Even at submillisecond exposure times, the proposed shutter would not pose any timing or jitter problems.

The proposed shutter could be used with any image sensor, including a 100-percent-fill-factor sensor, which is typically a high-end progressive-scan CCD. Heretofore, fast cameras have typically contained interline-transfer image sensors, which are less sensitive to red and infrared than standard CCDs. Thus, the user can obtain the advantage of the increased signal and increased red and infrared response of a 100-percent-fill-factor, progressive-scan focal-plane device, relative to an interline-transfer device.

The proposed shutter could also be utilized in time-resolved spectroscopy. This would involve (1) imaging a spectrum onto the array of mirrors, with the spectrometer slit oriented along the columns of mirrors and the spectrum along the rows of mirrors and (2) re-imaging the spectrum from the mirror plane onto the CCD array. The spectroscopic cycle would start with all mirrors in the "off" position, so there would be no image on the CCD. Then the mirrors would be switched momentarily to the "on" position, a few rows at a time, in succession across the array, yielding a succession of time-resolved spectra on the CCD.

This work was done by Gregory Bearman, Robert Green, Michael Eastwood, and Thomas Chrien of Caltech for **NASA's Jet Propulsion Laboratory**. *Further information is contained in a TSP [see page 1].*
NPO-20396

BLANK PAGE

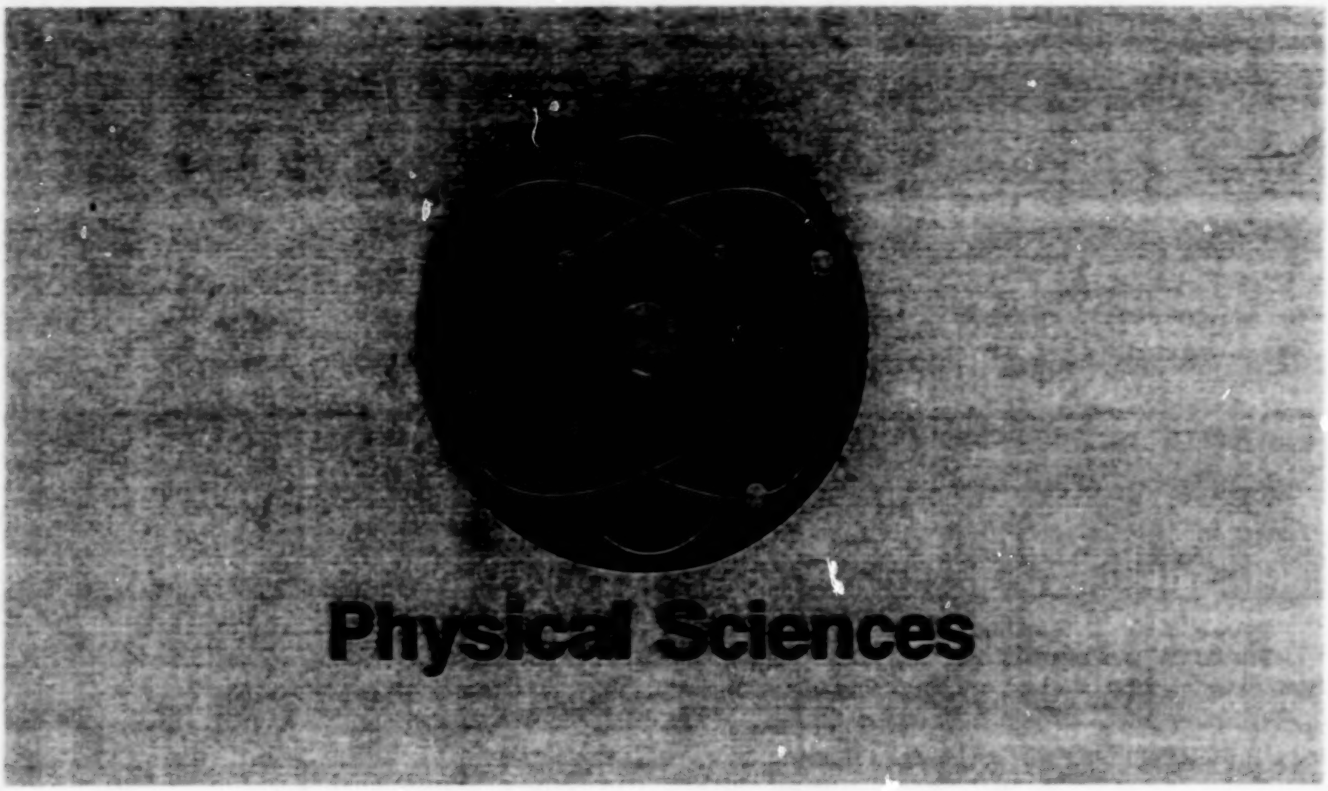

Hardware, Techniques, and Processes

BLANK PAGE

Passive Optical Measurement of Velocity in a Luminous Flow

Neither seeding nor illumination of the flow is necessary.

Lewis Research Center, Cleveland, Ohio

A segmented-image emission velocimeter (SIEVE) is an optical instrument for measuring the velocity of a luminous turbulent flow. More specifically, it measures a component of flow velocity perpendicular to its line of sight. This instrument is not only nonintrusive but is also passive in the sense that unlike other flow-measuring optical instruments, it does not seed the flow and does not illuminate the flow to obtain scattering of light from seed particles in the flow; instead, it utilizes broad-band light emitted by the flow. Flows amenable to SIEVE velocity measurement include flames and rocket exhaust plumes.

The operation of a SIEVE is based on a plasma-diagnostic technique developed in the 1970s. By use of a telescope and beam splitters, identical images of a small region in a luminous flow field are formed on two binary transmission gratings (see figure). The transparent and opaque strips in each grating are of equal width and oriented perpendicularly to the velocity component of interest. The strips in the two gratings are positioned 180° out of phase with each other along the velocity component; that is, each transparent strip of one grating coincides, in the image, with an opaque strip of the other grating. Light that strikes the transparent strips of each grating is focused onto an avalanche photodiode behind the grating.

Small inhomogeneities in the luminosity of the flow (typically associated with turbulence and/or with glowing soot particles) give rise to corresponding inhomogeneities in the patterns of light moving across the gratings. As a result, the output of each photodetector fluctuates. The outputs of the two photodiodes are amplified, then summed and differenced. Because of the complementarity of the gratings, the phase of the difference signal contains information on the motion of the light pattern across the gratings. Differencing also provides a high degree of common-mode rejection, making it possible to resolve small fluctuations in light emitted by the flow.

The sum and difference signals are digitized, then fast Fourier transformed to obtain a frequency (f) characteristic of the passage of the inhomogeneities across the gratings. Then the velocity component (v) of interest is calculated from $v = fD/M$, where D is the spatial period of a grating and M is the magnification of the image projected onto a grating.

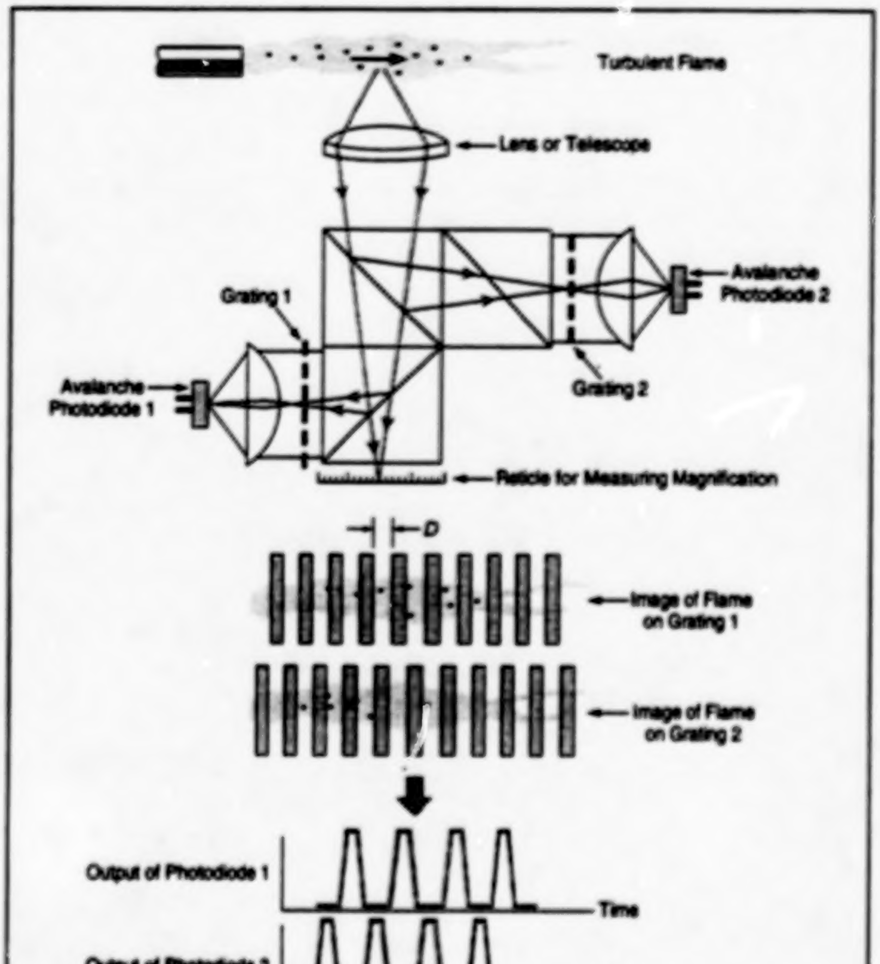

A Quasi-periodic Signal Is Generated from the difference between the outputs of the photodetectors behind the gratings. A fast Fourier transform of this signal yields a spectral peak, the frequency of which is proportional to the velocity component to be measured.

The response and noise characteristics of a prototype SIEVE were measured in tests in which an inhomogeneous luminous flow field of known velocity was simulated by use of a back-lighted transparent rotating wheel with a pitted surface. The prototype SIEVE was then used to measure velocities in flames from an oxyacetylene torch. The results of the measurements appeared to confirm that SIEVEs could be used to determine local velocities in turbulent, luminous flows. Further tests are expected to clarify the limitations and capabilities of SIEVEs.

This work was done by S. J. Schneider of **Lewis Research Center** *and S. F. Fulghum and P. S. Rostler of Science Research Laboratory, Inc. Further information is contained in a TSP [see page 1].*

Inquiries concerning rights for the commercial use of this invention should be addressed to NASA Lewis Research Center, Commercial Technology Office, Attn: Tech Brief Patent Status, Mail Stop 7–3, 21000 Brookpark Road, Cleveland, Ohio 44135. Refer to LEW-16637.

A Technique for Axial/Torsional Thermomechanical Fatigue Testing

Test conditions can be selected to approximate thermomechanical-loading conditions in engines.

Lewis Research Center, Cleveland, Ohio

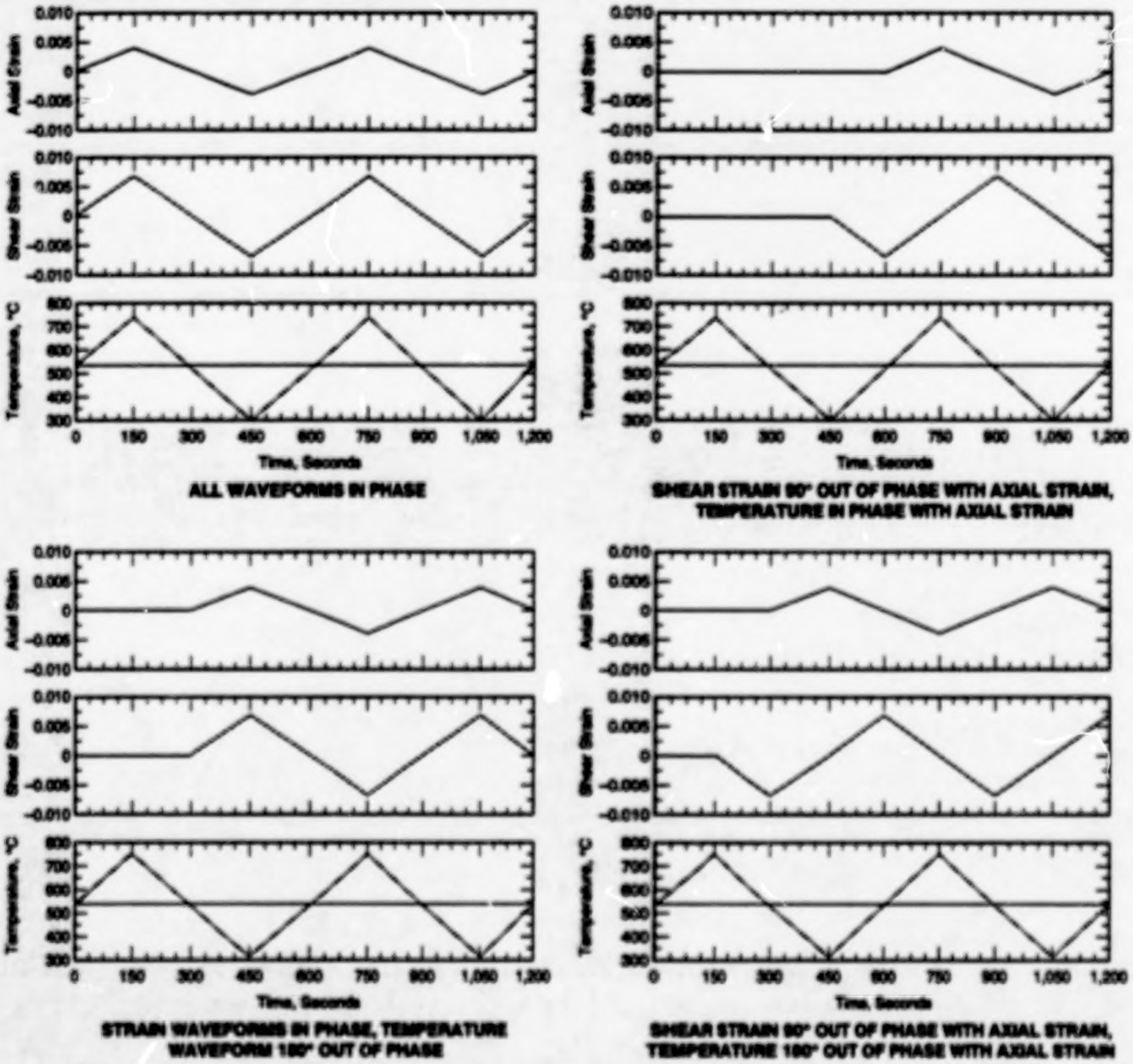

Figure 1. **Axial Strain, Shear Strain, and Temperature** are cycled with prescribed phase relationships.

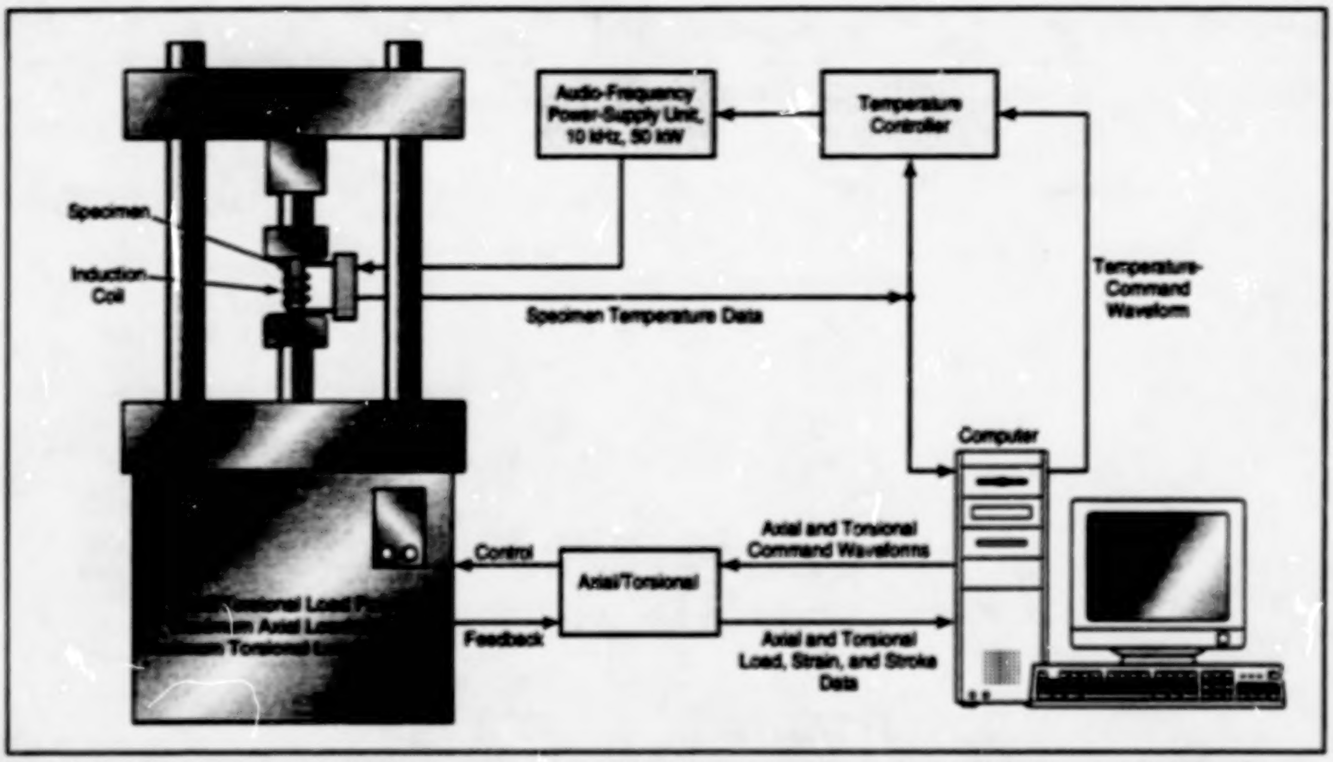

Figure 2. This Thermomechanical-Testing Apparatus was used to test tubular superalloy specimens with the thermomechanical loading conditions depicted in Figure 1.

A technique for thermomechanical fatigue testing of thin-walled tubular specimens involves the application of cyclic axial (tension/compression) and torsional (shear) strains, along with thermal cycling. In this technique, the phase relationships among the two strain waveforms and the temperature waveform are prescribed and are maintained constant throughout a test.

Heretofore, axial/torsional fatigue testing has commonly been limited to isothermal conditions, while thermomechanical fatigue testing has commonly been limited to axial (only) or torsional (only) strain. The present technique for axial/torsional thermomechanical fatigue (AT-TMF) testing makes it possible to acquire materials data on effects of time-varying thermal and multiaxial mechanical loads similar to those experienced by tubular components of engines during cyclic and/or transient operation. The data can be used, along with mathematical models of thermomechanical behavior, to predict the deformations and fatigue lives of such components.

In principle, one could choose among an infinite number of combinations of mechanical-strain and temperature waveforms; in practice, one must limit to the choice to a representative few. Four different combinations of triangular waveforms were chosen for the present AT-TMF testing technique. The waveforms in these combinations are required to be synchronized, variously, with 0°, 90°, and/or 180° phase differences. Figure 1 presents examples of the four combinations of waveforms. The cycle time and the temperature and strain limits in these examples are specific to tubular specimens (22 mm inner diameter, 26 mm outer diameter) of a cobalt-based superalloy; other limits and cycle times could be chosen to suit different specimens.

Figure 2 schematically depicts the apparatus that was used to implement the present AT-TMF testing technique on the specimens mentioned above. An axial/torsional load frame was controlled with two servocontrollers: one for the axial and one for the torsional actuator. The axial and shear strains were measured by a commercially available, water-cooled, axial/torsional extensometer. The specimen was heated by use of induction coils connected to a controllable audio-frequency power-supply unit rated at 50 kW.

The axial and torsional strains and temperature were controlled and test data were acquired by a computer system (equipped with digital-to-analog and analog-to-digital converters) connected to the servocontrollers, a temperature controller, and temperature sensors. The computer generated command waveforms that corresponded to the specified axial-strain, torsional-strain, and temperature waveforms. For each of 1,000 points during a test cycle, the computer acquired data on axial and torsional loads, strains, and strokes and on temperatures at five locations on the specimen. The computer operated with a C-language program that provided a keyboard interruption capability plus a graphical display of axial and shear stresses versus time, temperatures, and test status.

This work was done by Sreeramesh Kalluri and Christopher S. Burke of NYMA, Inc., and Peter J. Bonacuse of the Vehicle Propulsion Directorate of the U. S. Army Research Laboratory for **Lewis Research Center.** *Further information is contained in a TSP [see page 1].*

Inquiries concerning rights for the commercial use of this invention should be addressed to NASA Lewis Research Center, Commercial Technology Office, Attn: Tech Brief Patent Status, Mail Stop 7–3, 21000 Brookpark Road, Cleveland, Ohio 44135. Refer to LEW-16663.

FT-IR Measurement of Hydraulic Fluids in Perchloroethylene

Very low concentrations can be measured to verify cleanliness of hardware.

John F. Kennedy Space Center, Florida

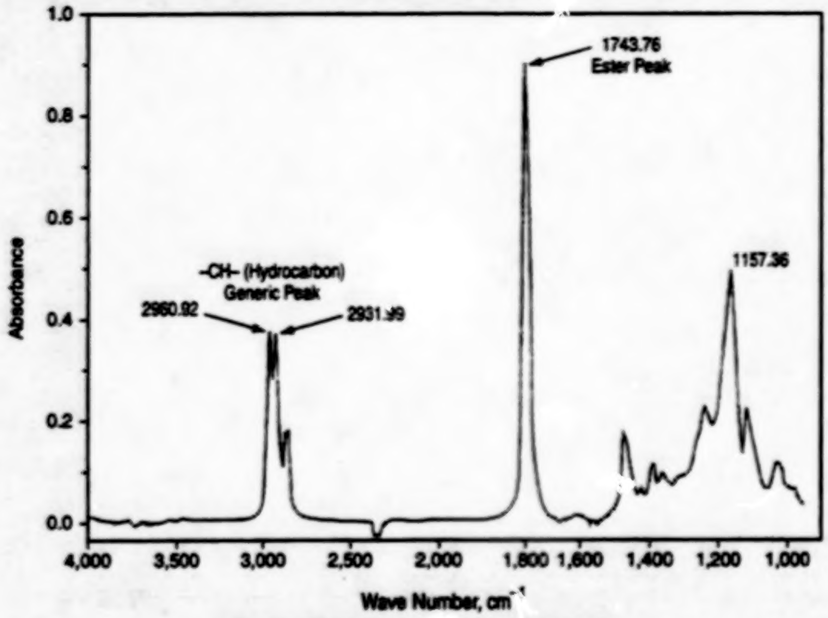

INFRARED SPECTRUM OF A TYPICAL ESTER-BASED INDUSTRIAL HYDRAULIC FLUID IN PERCHLOROETHYLENE

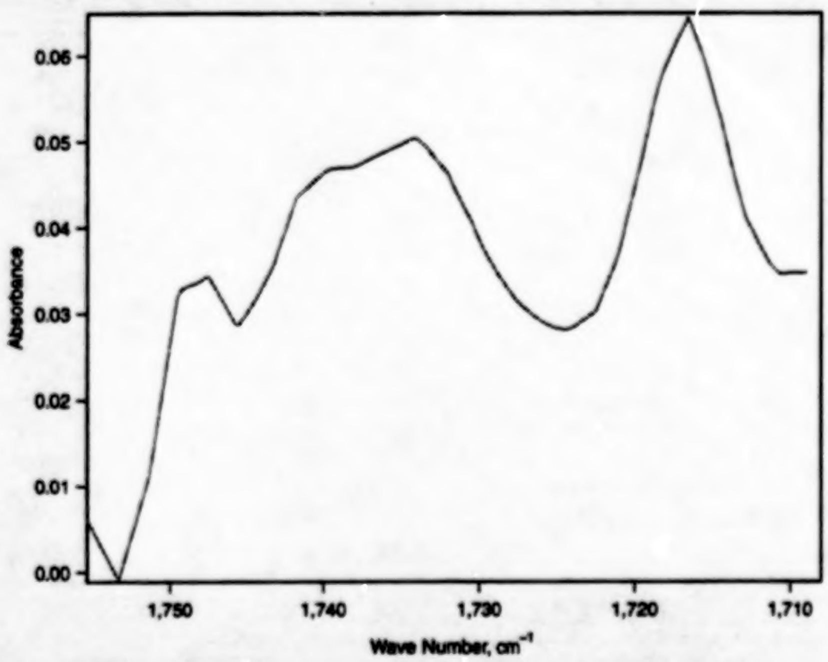

SPLITTING OF ESTER PEAK OF A MIXTURE OF HYDRAULIC FLUIDS DISSOLVED IN PERCHLOROETHYLENE AT A CONCENTRATION OF 19.9 mg/L

The Infrared Absorbance Spectrum of a perchloroethylene solution can be analyzed to find a peak characteristic of C=O ester groups in small amounts of greasy and oily residues dissolved in the solution.

An improved solvent-extraction/infrared-analysis technique has been devised to replace an older technique for measuring very small concentrations of nonvolatile residues of industrial hydraulic fluids, oils, and greases on hardware that is required to be cleansed of such residues. The older technique involves solvent extraction of nonvolatile residues followed by gravimetric determination of the quantity of dissolved residues.

The older technique entails two major disadvantages: The first disadvantage is that the solvent is 1,1,2-trichloro-1,2,2-trifluoroethane (also known by the trade name "Freon 113"). This and other chlorofluorocarbons have been found to contribute to depletion of ozone in the upper atmosphere, and therefore the law requires that they be phased out of production and use. The second major disadvantage is that the gravimetric method is susceptible to large errors at the low concentrations of interest in the original application. In terms of areal mass density on the hardware, these concentrations are typically a few milligrams per square foot (1 mg/ft^2 ≈ 11 mg/m^2); in terms of volume mass densities in solution, these concentrations are typically a few milligrams per liter.

The improved solvent-extraction/infrared-analysis technique features (1) the use of a less-harmful solvent and of (2) Fourier-transform infrared (FT-IR) analysis of an infrared spectral peak specific to the dissolved residues that one seeks to detect. The solvent in this technique is perchloroethylene; in comparison with 1,1,2-trichloro-1,2,2-trifluoroethane, perchloroethylene is relatively environmentally benign and nontoxic. Perchloroethylene is also less volatile; it boils at a temperature of 121 °C, whereas 1,1,2-trichloro-1,2,2-trifluoroethane boils at 48 °C.

The spectral peak in question is one attributable to ester C=O groups conjugated with C=C groups or aromatic rings in organic molecules. This ester peak is suitable because even at relatively low spectral resolution, it stands out from other spectral peaks attributable to C-H bonds (see upper part of figure) and because the residues of interest contain such ester C=O groups. With higher spectral resolution, the ester peak of a typical residue of interest dissolved in perchloroethylene can be seen to be split into two peaks: one at wave numbers from ~1,753 to ~1,724 cm^{-1} and one at wave numbers from ~1,724 to ~1,708 cm^{-1} (see lower part of figure). The splitting has been conjectured to be caused by interactions between the residue and perchloroethylene molecules.

The technique has been tested in experiments on solutions of various industrial

hydraulic fluids dissolved in perchloroethylene at known concentrations. The solutions were analyzed on an apparatus that comprised a standard high-intensity infrared source, a Fourier-transform infrared (FT-IR) spectrometer containing a Michelson interferometer, and an HgCdTe photodetector cooled by liquid nitrogen. The output of the spectrometer was digitized and processed by a spectral-analysis computer program. The results of the experiments were interpreted as signifying that the ester spectral peaks can indicate the presence of the residues of interest at the low concentrations of interest, and that at areal concentrations as low as ~1 to ~5 mg/ft^2 (~11 to ~54 mg/m^2), the areas under the two ester spectral peaks are indicative of the concentrations within a factor of 2.

This work was done by Narinder K. Mehta of the University of Puerto Rico for **Kennedy Space Center**. *Further information is contained in a TSP [see page 1].* *KSC-11945*

Metal/Dielectric-Film Interference Color Filters

These filters could be fabricated at relatively low cost.

NASA's Jet Propulsion Laboratory, Pasadena, California

Color interference filters for individual pixels in solid-state electronic image and display devices would be made of thin metal and dielectric films, according to a proposal. The proposed filters would overcome the primary disadvantage (high cost) of dye color filters like those used in liquid-crystal display devices, digital cameras, and camcorders. The proposed filters would also offer advantages of cost and functionality over color interference filters made of alternating dielectric layers with different indices of refraction.

The all-dielectric filters are expensive because of the need for large numbers of layers to obtain adequate discrimination among red, green, and blue (RGB). The proposed filters would provide adequate color discrimination with acceptably broad-band response (pass wavelength bands about 100 nm wide). The proposed filters would be relatively inexpensive because they would contain fewer layers — typically no more than five layers, and only two layers need to have different thickness for RGB colors, which means it only needs to be masked $2 \times (3 - 1) = 4$, as contrasted with more than 10 layers for an all-dielectric filter, and needs to be masked $10 \times (3 - 1) = 20$.

Figure 1 shows aspects of a proposed five-layer metal/dielectric filter containing three layers of silver alternating with two layers of magnesium fluoride. The table in the figure shows the film thicknesses needed to make the filter transmit each of the three primary colors. The corresponding silver layers for all three color filters could be of the same thicknesses; only the magnesium fluoride layers would differ in thickness among the three colors. The total number of distinct layer thicknesses is only five, three for silver and two for magnesium fluoride.

Because of the small number of thicknesses, patterning and other aspects of the fabrication of a device with three primary-color filters in each pixel (see Figure

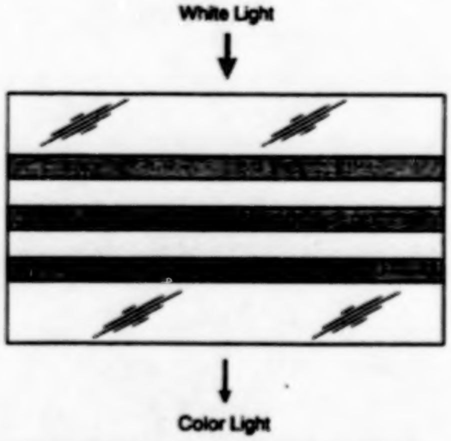

CROSS SECTION OF FILTER (NOT TO SCALE)

	Ag	MgF_2	Ag	MgF_2	Ag
Red	23	185	40	185	23
Green	23	150	40	150	23
Blue	23	110	40	110	23

LAYER THICKNESSES (IN NANOMETERS) FOR TRANSMITTING EACH OF THE PRIMARY COLORS

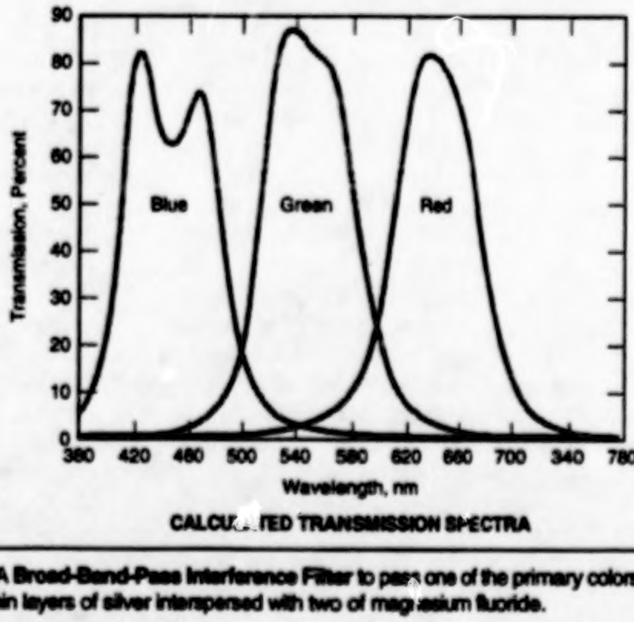

CALCULATED TRANSMISSION SPECTRA

Figure 1. A **Broad-Band-Pass Interference Filter** to pass one of the primary colors could be made of three thin layers of silver interspersed with two of magnesium fluoride.

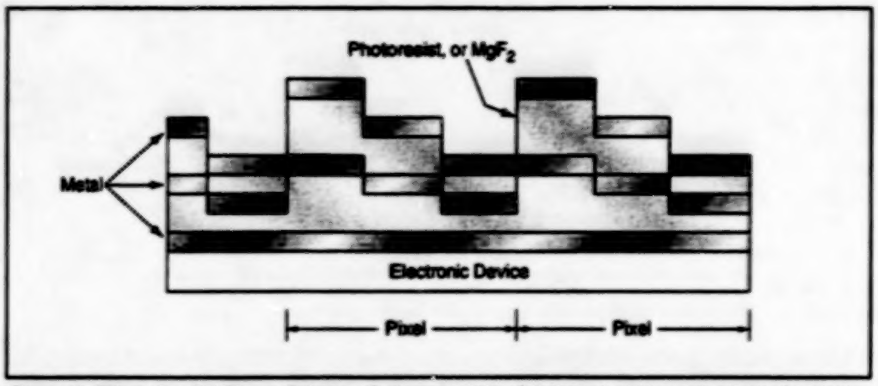

Figure 2. Filters for All Three Primary Colors could be fabricated within each pixel of a display or image device, by use of established deposition and photoresist patterning techniques.

2) would be relatively easy. The metal patterns could be formed in the presence of photoresist masks temporarily substituting for the magnesium fluoride films. The optical thickness of each photoresist mask would be made equal to that of the magnesium fluoride film to be subsequently deposited in its place. Because it is relatively easy to control the thickness of a photoresist mask, fabrication should be relatively simple and inexpensive.

This work was done by Yu Wang of Caltech for **NASA's Jet Propulsion Laboratory.** *Further information is contained in a TSP [see page 1].*

In accordance with Public Law 96-517, the contractor has elected to retain title to this invention. Inquiries concerning rights for its commercial use should be addressed to

Technology Reporting Office
JPL
Mail Stop 122-116
4800 Oak Grove Drive
Pasadena, CA 91109
(818) 354-2240

Refer to NPO-20217, volume and number of this NASA Tech Briefs *issue, and the page number.*

Optoelectronic Liquid-Level Gauges for Aircraft Fuel Tanks

Replacement could be accomplished in minutes instead of days.

NASA's Jet Propulsion Laboratory, Pasadena, California

Gauges that would measure liquid levels optically have been proposed for use in aircraft fuel tanks. These gauges would contain no moving parts (no floats) and no wiring inside the tanks. Their overall function could be characterized as that of permanently immersed, self-reading dipsticks.

The proposed gauges are intended to supplant the capacitance probes now used to measure liquid-fuel levels in such tanks. Capacitance probes are mounted at several locations inside a tank and are connected to external instrumentation via wiring. The probes and wiring are usually reliable, but fail occasionally. Because replacement of capacitance probes and/or wiring involves intrusion into the tank, the aircraft could be out of service for days.

In a gauge of the proposed type, the only part intruding into the tank would be a rodlike assembly, mounted from the outside of the tank, that would provide optical access to the liquid inside. The rodlike assembly would include a baffle plus a rod made of a suitable transparent material. The rod would be etched or scored at prescribed intervals along its length to provide optically reflective fiducial marks at known levels. Light would be coupled into the rod from a source at the outer end to illuminate the fiducial marks. A camera or other imaging device would be mounted adjacent to the source of light and would be aimed along the rod to observe the illuminated marks.

The rod material would be chosen so that its index of refraction would approximately match that of the liquid in the tank. As a result, the fiducial marks immersed in the liquid would appear dark to the imaging device, while those above the surface of the liquid would appear bright to the imaging device. The liquid level would thus be assumed to lie between the lowest bright mark and the dark mark just below it. The output of the imaging device would be processed to into an indication of the liquid level in increments of depth between fiducial marks.

A mass-produced gauge of this type would likely include a miniature imaging device containing an active-pixel sensor, plus input/output circuits, all integrated on a single chip. An application-specific integrated circuit (ASIC) for processing the image-sensor output could also be included. Clock and command signals and signal input voltage would be supplied to the chip from external instrumentation. The overall size of the unit on the outer end of the rod assembly (including the ASIC) would be of the order of 1 in.^{3} ($\approx$16 cm^3).

In a typical case, it would be necessary to place gauges at several locations. Then the fuel-level readings from the several locations could be processed by an algorithm that would take account of the shape of the tank in determining the amount of fuel remaining. It should also be possible to implement some form of autocalibration in software. The level readings or the final calculated quantity of fuel could be integrated or averaged before being displayed in nearly real time (update every few seconds).

With respect to initial costs, the proposed gauges would be competitive with capacitive fuel gauges. However, recurring costs of the proposed gauges would be much lower because their rodlike assemblies could be replaced in minutes instead of days.

This work was done by Philip Moynihan, Paul Henry, Tien-Hsin Chao, William Lincoln, William King, and Lloyd Adams of Caltech for **NASA's Jet Propulsion Laboratory.** *Further information is contained in a TSP [see page 1].*
NPO-20105

Shape-Memory-Alloy Thermal-Conduction Switches

These devices would be simple, cheap, and reliable.

NASA's Jet Propulsion Laboratory, Pasadena, California

Variable-thermal-conduction devices containing shape-memory-alloy (SMA) actuators have been proposed for use in situations in which it is desired to switch on (or increase) thermal conduction when temperatures rise above specified values and to switch off (or decrease) thermal conduction when temperatures fall below those values. The proposed SMA thermal-conduction switches could be used, for example, to connect equipment to heat sinks to prevent overheating, and to disconnect the equipment from heat sinks to help maintain required operating temperatures when ambient temperatures become too low. In comparison with variable-conductance heat pipes and with thermostatic mechanisms that include such components as bimetallic strips, springs, linkages, and/or louvers, the proposed SMA thermal-conduction switches would be simple, cheap, and reliable.

The basic design and principle of operation of an SMA thermal-conduction switch is derived from an application in which thermal conduction from hot components to a cooling radiator takes place through the contact area of bolted joints. The thermal conductance depends on the preload in each joint. One could construct an SMA thermal-conduction switch by simply mounting an appropriately designed SMA washer under the bolthead. As the temperature falls below (or rises above) the SMA transition temperature, the SMA washer would contract (or expand) axially by an amount sufficient to unload (or load) the bolt, thereby shutting off (or turning on) most of the thermal conduction through the joint contact area. SMA washers with various transition temperatures can be made to suit specific applications.

This work was done by Virginia Ford and Richard Parks of Caltech for **NASA's Jet Propulsion Laboratory**. *Further information is contained in a TSP* *[see page 1]*.

NPO-20437

Pressurization and Leak Testing of Sample-Return Canisters

Sealed canisters would be pressurized with a radioactive gas.

NASA's Jet Propulsion Laboratory, Pasadena, California

A technique that involves pressurization with a radioactive gas has been proposed to solve two problems associated with canisters used to transport samples from remote bodies (planets, moons, asteroids, or comets) back to Earth. The canisters must be sealed at the sampling locations. The problems are how to test the canisters for leakage during transit and how to prevent buckling of the containers from the onset of atmospheric pressure upon return to Earth. The solution to these problems could also be adapted to use on Earth to ensure the integrity of canisters used to store material specimens for long times and to prevent the collapse of sealed canisters that must be brought to or stored at pressures higher than those at which the samples are sealed inside.

According to the proposal, a small container of radioactive krypton (mixed with another suitable pure gas or mixture of gases) would be placed in each sample canister. The container of gas would be equipped with means to release the gas into the interior of the canister soon after the canister is hermetically sealed with the sample inside. A Geiger counter or other radioactivity sensor near the canister would provide an indication of the leakage (if any) of radioactive gas from the canister. The amount of gas provided must be large enough so that the pressure in the canister is sufficient to resist buckling of the canister under ambient atmospheric pressure.

This work was done by Joseph C. Lewis of Caltech for **NASA's Jet Propulsion Laboratory**. *No further documentation is available.*

NPO-20446

BLANK PAGE

32

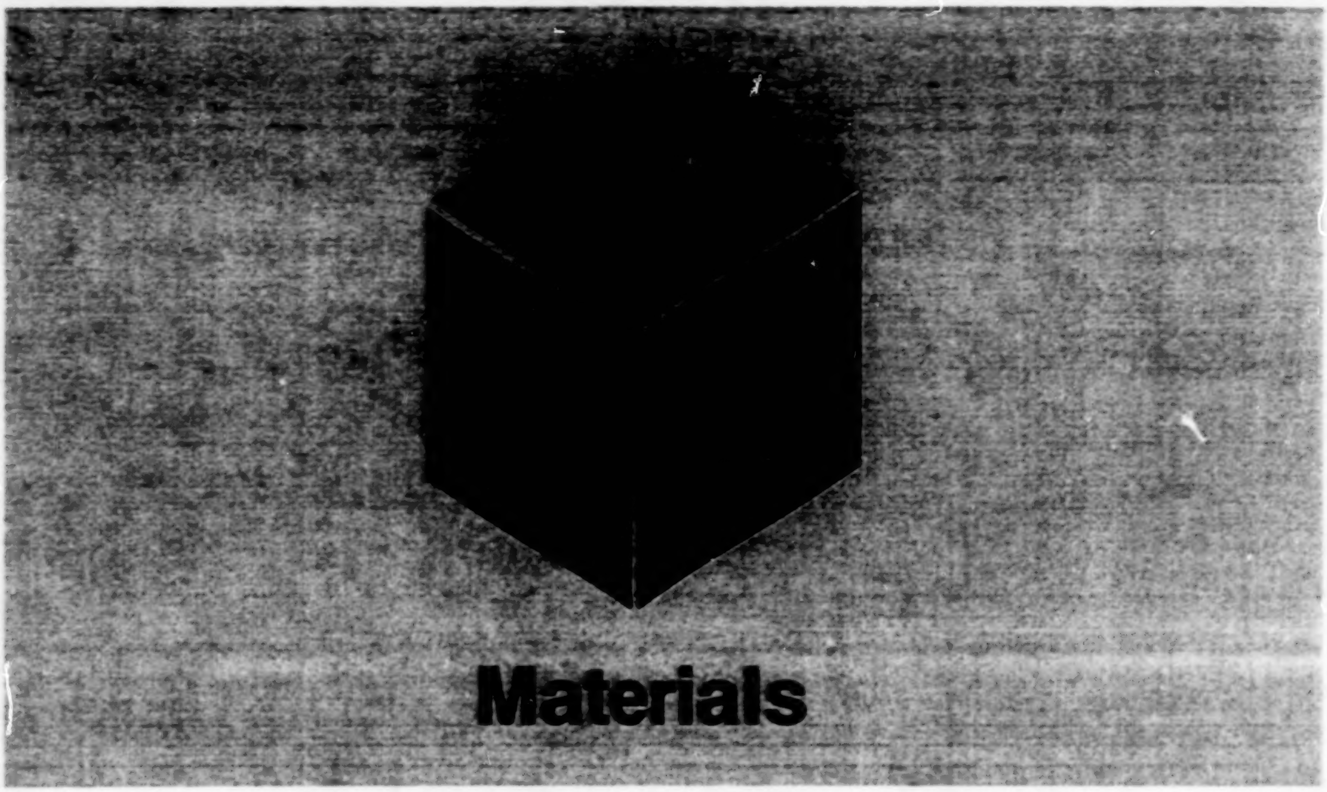

Hardware, Techniques, and Processes

BLANK PAGE

24

High-Performance Thermoelectric Materials Based on β-Zn_4Sb_3

Even better performances are obtained with solid solutions of β-Zn_4Sb_3 and Cd_4Sb_3.

NASA's Jet Propulsion Laboratory, Pasadena, California

Materials based on β-Zn_4Sb_3 have been found to exhibit unusually high values of the dimensionless thermoelectric figure of merit at temperatures between 200 and 400 °C. The discovery that p-type β-Zn_4Sb_3 is a high-performance thermoelectric material is reported in "Zn_4Sb_3: A High-Performance Thermoelectric Material" (NPO-19677), (following article). The development reported here extends beyond that discovery to include solid solutions of Zn_4Sb_3 and Cd_4Sb_3 (with general compositions given by $Zn_{4-x}Cd_xSb_3$) in the class of high-performance thermoelectric materials based on β-Zn_4Sb_3.

The development has included studies of doping with impurities and of deviation from stoichiometry as means to affect the electrical properties of β-Zn_4Sb_3. These studies have included the preparation of samples with electrical conductivities of both the p- type and the n-type. Theoretical modeling of the thermoelectric properties of p-type β-Zn_4Sb_3 was also performed to predict the maximum achievable figure of merit for this compound as a function of temperature, and experimental values were found to approach the predicted values.

The thermoelectric figure of merit, ZT is given by $ZT = \alpha^2T/\rho\lambda$, where α is the Seebeck coefficient, T is the absolute temperature, ρ is the electrical resistivity, and λ is the thermal conductivity. The figure illustrates ZT as a function of temperature, both from the theoretical prediction described above and as calculated from measurements on p-doped β-Zn_4Sb_3, on other state-of-the-art p-doped thermoelectric materials, and on a p-type Zn_4Sb_3/Cd_4Sb_3 solid solution of nominal composition $Zn_{3.2}Cd_{0.8}Sb_3$. In the cited prior article, the high ZT of p-type β-Zn_4Sb_3 in the temperature range of interest was attributed partly to its low thermal conductivity, which was then the lowest known thermal conductivity of any thermoelectric material in that temperature range. Since then, the thermal conductivity of the $Zn_{3.2}Cd_{0.8}Sb_3$ solid solution has been found to be even lower. The net result is that the ZT values of $Zn_{3.2}Cd_{0.8}Sb_3$ exceed those of β-Zn_4Sb_3 at temperatures > 50 °C, reaching a high value of 1.4 at a temperature of 250 °C.

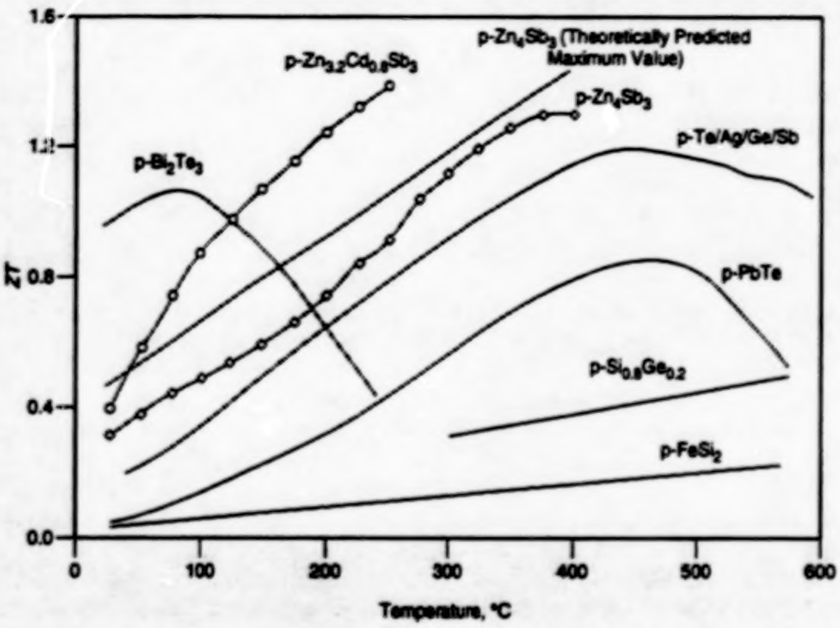

The Dimensionless Figure of Merit (ZT) of $Zn_{3.2}Cd_{0.8}Sb_3$ exceeds that of β-Zn_4Sb_3, and exceeds the ZTs of other thermoelectric materials even more.

Temperature-stability tests have shown that thermoelectric materials based on β-Zn_4Sb_3 are stable in dynamic vacuum at temperatures up to about 250 °C and in static vacuum up to about 400 °C. A Zn/Cd eutectic brazing material has been developed for use in bonding these materials to copper electrodes. Contact electrical resistivities between samples of these materials and copper electrodes have been found to be very low. Thus, it should be relatively easy to incorporate these materials into thermoelectric power-generating and cooling devices.

This work was done by Thierry Caillat, Alexander Borshchevsky, and Jean-Pierre Fleurial of Caltech for **NASA's Jet Propulsion Laboratory**. *Further information is contained in a TSP (see page 1).*

In accordance with Public Law 96-517, the contractor has elected to retain title to this invention. Inquiries concerning rights for its commercial use should be addressed to

Technology Reporting Office
JPL
Mail Stop 122-116
4800 Oak Grove Drive
Pasadena, CA 91109
(818) 354-2240

Refer to NPO-19851, volume and number of this NASA Tech Briefs *issue, and the page number.*

Zn_4Sb_3: A High-Performance Thermoelectric Material

The thermoelectric figure of merit at 200 to 350 °C is the greatest known.

NASA's Jet Propulsion Laboratory, Pasadena, California

Zn_4Sb_3 has been identified as a high-performance thermoelectric material. In p-type, Zn_4Sb_3 samples have exhibited the greatest dimensionless thermoelectric figure of merit ever observed for a p-type material at temperatures from 200 to 350 °C. In this respect, Zn_4Sb_3 fills a gap in the thermoelectric-performance spectrum between the state-of-the-art thermoelectric materials like (a) p-type Bi_2Te_3-based alloys, which exhibit their greatest figures of merit at lower temperatures and (b) p-type

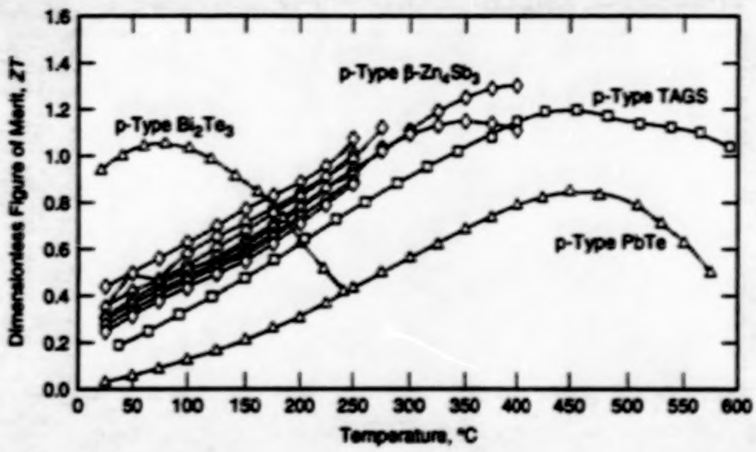

The Values of the Dimensionless Figure of Merit of samples of β-Zn_4Sb_3 **in the temperature range of 200 to 350 °C were found to exceed those of other thermoelectric materials.**

Te/Ag/Ge/Sb ("TAGS") alloys and p-type PbTe-based alloys, which exhibit their greatest figures of merit at higher temperatures. Thus, Zn_4Sb_3 offers an important thermoelectric-performance advantage for generating electrical energy from heat sources in the temperature range from 200 to 350 °C. Zn_4Sb_3 also costs less than do the state-of-the-art lower- and higher-temperature alloys.

Zn_4Sb_3 exists in three phases; α (which is stable below −10 °C), β (which is stable from −10 to 492 °C), and γ (which is stable from 492 °C to the melting temperature of 566 °C). In the temperature range of interest, Zn_4Sb_3 thus manifests itself as β-Zn_4Sb_3, which has been reported in the literature to be characterized by a band gap of about 1.2 eV. Single crystals of β-Zn_4Sb_3 were prepared by the Bridgman gradient-freeze technique. In addition, polycrystalline samples were prepared by melting and direct reaction of powders of Zn and Sb followed by regrinding of the resulting ingots into powder followed by hot pressing to consolidate the powders into solid pellets.

The thermoelectric properties of the crystalline and polycrystalline samples were measured and found to be similar. The results show that β-Zn_4Sb_3 is a heavily-p-doped semiconductor. The dimensionless thermoelectric figure of merit, ZT is defined by $ZT = \alpha^2T/\rho\lambda$, where α is the Seebeck coefficient, T is the absolute temperature, ρ is the electrical resistivity, and λ is the thermal conductivity. The figure illustrates ZT as a function of temperature as calculated from the measurements on the β-Zn_4Sb_3 samples, plus ZT as a function of temperature for the state-of-the-art thermoelectric materials mentioned previously. One of the most interesting features of β-Zn_4Sb_3 that contributes to its relatively large ZT is its thermal conductivity, which reaches a low value of only 6 mW/(cm·K) at 250 °C. This is the lowest thermal conductivity of any thermoelectric material known thus far.

There are many potential applications for β-Zn_4Sb_3 in thermoelectric generators, especially for recovering electrical energy from waste heat. Sources that generate waste heat in the temperature range of peak thermoelectric performance of β-Zn_4Sb_3 include garbage incinerators, geothermal sources (including hot oil from oil wells), power plants, and automobiles.

This work was done by Thierry Caillat of Caltech for **NASA's Jet Propulsion Laboratory**. *Further information is contained in a TSP [see page 1].*

In accordance with Public Law 96-517, the contractor has elected to retain title to this invention. Inquiries concerning rights for its commercial use should be addressed to

Technology Reporting Office
JPL
Mail Stop 122-116
4800 Oak Grove Drive
Pasadena, CA 91109
(818) 354-2240

Refer to NPO-19677, volume and number of this NASA Tech Briefs *issue, and the page number.*

Cold Hibernated Elastic Memory (CHEM) Expandable Structures

Compacted structures would be deployed with heat only.

NASA's Jet Propulsion Laboratory, Pasadena, California

Experiments have confirmed the feasibility of a new class of lightweight, reliable, simple, and low-cost expandable structures. The concept called "cold hibernated elastic memory" (CHEM) utilizes the shape memory polymers (SMPs) in open cellular structures. Basically, these structures are SMP foams that are under development by Jet Propulsion Laboratory (JPL) and Mitsubishi Heavy Industry (MHI).

In CHEM concept, the structures of any shape, such as rods, tubes, wheels, boards, chassis, packages, tanks, and the like, are fabricated from larger SMP foam blocks. Subsequently, they are compacted to very small volumes in rubbery (flexible) state above the glass-transition temperature (T_g) and later cooled below T_g to glassy state. When the stowed structure is frozen, the external compacting forces are removed and the part can be stowed in cold hibernated state for unlimited time below T_g. A compacted part can be heated above T_g to rubbery state and the original shape will be precisely restored by simultaneous elastic recovery of the foam and its shape-memory polymer effect. A fully deployed structure can be rigidized by cooling below T_g to glassy state. Once deployed and rigidized, a part could be heated and recompacted. In principle, there should be no limit on achievable number of compaction/deployment/rigidization cycles.

The main advantages of the CHEM structures over conventional polymer foams are as follows:

- Both elastic and plastic compressive strains are precisely recovered;
- High full/stowed volume ratios are achieved;
- High ratios of elastic modulus (E) below T_g to E above T_g allow to keep original shape in stowed, hibernated condition, without external compacting forces;
- Small temperature range for full transformation from rigid to rubbery state reduces the heat consumption during deployment (shape restoration);
- Wide range of T_g from −70 to +100 °C

results in many applications.

Advantages over other expandable/deployable structures are as follows:

- high reliability,
- low cost,
- simplicity,
- no deployment/inflation systems,
- clean deployment and rigidization,
- none or very little long-term stowage effects, and
- inexpensive technology development.

The disadvantage of CHEM structure is that heat energy is needed for deployment. However, natural heat sources are considered to be utilized and studies/proof-of-concept are planned to be conducted.

A wide range of T_g from −70 to +100 °C results in a myriad possible space and terrestrial commercial applications. The CHEM concept could be applied to shelters, hangars, camping tents or outdoor furniture, to mention just a few. Such articles could be made of an SMP foam with a T_g slightly above the highest outdoor summer temperature. The CHEM parts can be transported and stored in small packages, then expanded by heating at the outdoor site. After expansion, the CHEM parts will be allowed to cool to ambient temperature below their T_g and rigidize.

This work was done by Witold Sokolowski and Artur Chmielewski of Caltech for **NASA's Jet Propulsion Laboratory**. *Further information is contained in a TSP [see page 1].*

NPO-20394

Nonchromic Acid Brightener for Brass and Copper

A process for precleaning brass and copper parts before processing them further in a clean room includes a brightening chemical treatment in solution of 85 volume percent phosphoric acid, 3 volume percent nitric acid, and 12 volume percent acetic acid. This solution acts rapidly and can be discarded easily; it replaces a chromic-acid brightening solution that has become subject to environmental regulation. In preparation for the treatment, a part is first alkaline cleaned, rinsed with water, and dried until no water is visible. The part is then treated by immersing it in the solution for 10 seconds or until bubbles appear on all its surfaces. The part is then rinsed with water and dried.

This work was done by Paul H. Biesinger of AlliedSignal, Inc., for **Johnson Space Center**. *No further documentation is available.*

MSC-22662

38

BLANK PAGE

Mechanics

Hardware, Techniques, and Processes

BLANK PAGE

Inflatable Strakes for Forebody Vortex Control

It is not necessary to allocate valuable forebody volume to strake-deployment mechanisms.

Ames Research Center, Moffett Field, California

Inflatable nose strakes have been invented to assist in controlling the direction of flight of an airplane, especially a high-performance fighter-type airplane operating at a high angle of attack. In general, adjustments of the sizes, shapes, positions, and/or orientations of nose strakes gives rise to variations in forebody vortices and, consequently, to variations in aerodynamic forces. These variations can be used for flight control. Hinged, rigid nose strakes controlled by mechanical actuators via linkages have been investigated for use in forebody vortex control for flight control, but they entail a significant disadvantage; the actuators and linkages occupy valuable forebody interior volume that is needed for radar and other instrumentation. In contrast, inflatable nose strakes occupy much less forebody interior volume.

Figure 1 depicts a typical fighter-type airplane at a high angle of attack, equipped with inflatable nose strakes. Each inflatable forebody strake includes an inflatable elastic polymeric membrane mounted in a shallow recess in exterior skin of the forebody. The membrane is held in place by a clamping frame around the edge of the recess. A fluid coupling provides an opening into the volume enclosed by the membrane, for inflation or deflation of the membrane.

When the strakes are not inflated, the outer surfaces of the membranes lie flush with the adjacent forebody surface. When either strake is inflated, the outer surface of the membrane protrudes into the airflow, affecting the forebody vortices. If the strake on the right or left side of the forebody is inflated, the effect on the vortices is such as to give rise to a net leftward or rightward force, thereby causing the airplane to yaw to the left or right, respectively. If the membranes on both sides are inflated equally, the net effect is to generate a longitudinal or a pitch control force.

Figure 2 is a schematic diagram of the system for controlling the inflatable strakes. Any suitable pressurized fluid can be used to inflate the membranes; ordinarily, the preferred fluid is air because it can be handled easily, using equipment that adds little to the overall weight of the airplane. The pressurized air can be obtained via a tap from the airplane engine or from a separate compressor. A valve directs the flow of the pressurized fluid to neither, either, or both strakes. The pilot controls the valve through the airplane flight-control system.

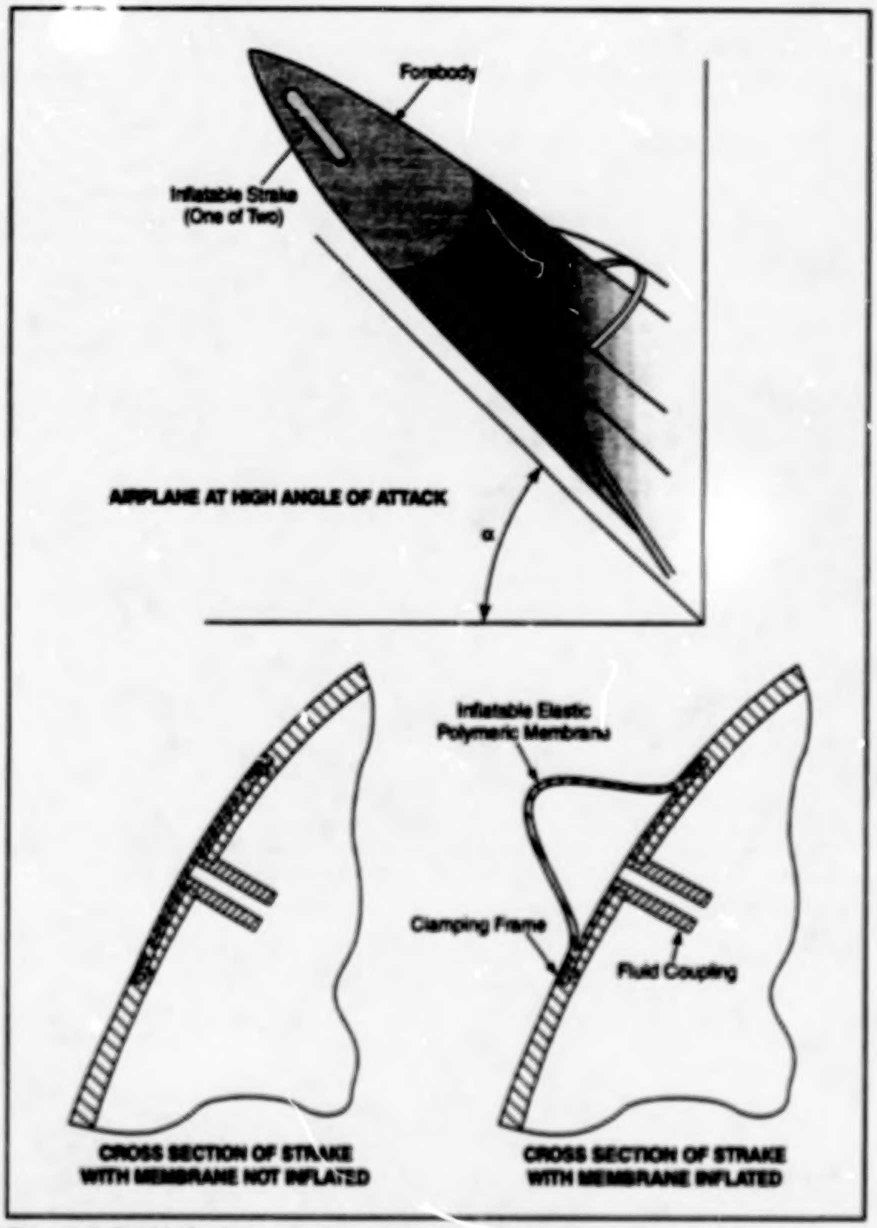

Figure 1. **Inflatable Strakes** on the right and left sides of the forebody provide additional degrees of flight control, beyond that of conventional flight-control surfaces.

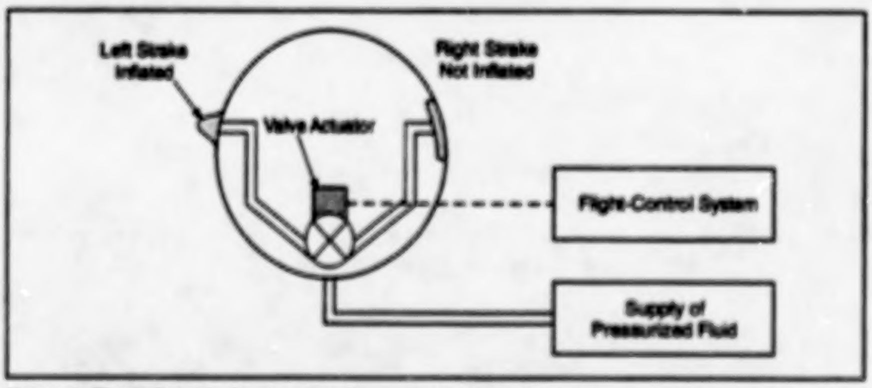

Figure 2. **The Inflatable Strakes Are Controlled** by a lightweight, compact pneumatic system, instead of by mechanical actuators and linkages like those used to control rigid strakes.

This work was done by Peter T. Zell of **Ames Research Center**. *Further information is contained in a TSP [see page 1].*

This invention has been patented by NASA (U.S. Patent No. 5,326,050). Inquiries concerning nonexclusive or exclusive license for its commercial development should be addressed to the Patent Counsel, Ames Research Center [see page 1]. Refer to ARC-11979.

Analysis of Flutter of the APEX Sailplane

This airplane is expected to be safe from destruction by flutter instabilities.

Dryden Flight Research Center, Edwards, California

Figure 1. The **APEX Sailplane**, shown here as rendered by an artist, would be a unique, remotely piloted research airplane that would fly at high altitudes.

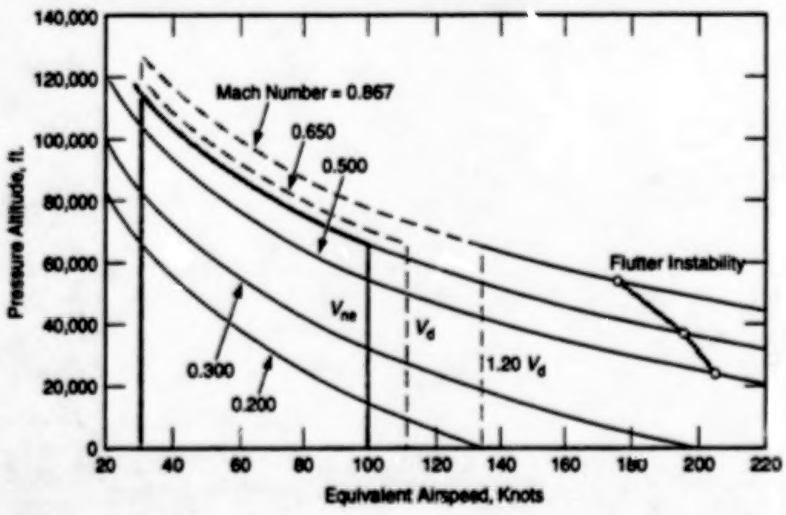

Figure 2. The **APEX Flight Envelope** does not enclose any flutter instability, according to flutter analysis. (V_{ne} = Velocity never exceed; V_d = Velocity in dive.)

The proposed APEX high-altitude aerodynamical-research sailplane (see Figure 1) has been predicted to be free of flutter instabilities within its flight envelope. Designed to fly under remote control at altitudes of up to 100,000 ft (30.5 km), the APEX airplane would feature a stiff boron composite structure, the vibration-mode characteristics of which would be such that they should enable the airplane to fly at relatively high subsonic mach numbers without risk of destruction by flutter.

This prediction is the product of a flutter analysis that included a modal analysis based on a mathematical model of the dynamics of the airplane structure. Modal analysis is an essential part of flutter analysis; it is also needed in analysis of results of ground vibration tests and in the development of control laws. The flutter analysis was performed in lieu of flight tests to provide assurance of flutter stability, which tests are beyond the scope of the APEX project.

In preparation for the flutter analysis, the Advanced Soaring Concepts mathematical model of the structural dynamics was converted from a format denoted "COSMOS" to a format denoted "STARS" and validated. Detailed and accurate mass and stiffness distributions were included in the model.

The results of modal analyses were examined and plotted, and deflections were interpolated. Final flutter solutions were computed by use of a matched point, so that the flutter-stability calculations could be confirmed by recalculating them with flow parameters at the predicted stability boundary. The updated results of modal analysis were found to follow reasonable patterns. Flutter instabilities were found to lie well outside the flight envelope (see Figure 2).

This work was done by Roger Truax of **Dryden Flight Research Center**. *Further information is contained in a TSP [see page 1].*
DRC-98-74

Coupling Fixture Aligns and Seals Ends of Two Tubes

Inner diameters are matched and aligned to present a smooth surface to flow.

Lewis Research Center, Cleveland, Ohio

The figure presents a partial cross section of two poly(methyl methacrylate) (PMMA) tubes with machined ends butted and sealed together in a special coupling fixture. This coupling scheme, in conjunction with the careful selection of PMMA tubes to match inner diameters, ensures the precise alignment of the inner tube surfaces. The scheme was devised to satisfy a requirement in a liquid-flow experiment to ensure a smooth, continuous inner tube surface to prevent both flow disturbances and trapping of bubbles. If the inner diameters were not matched and/or the inner tube surfaces not aligned precisely, the junction between the tubes would feature small, sharp corners that could give rise to waves and could trap bubbles.

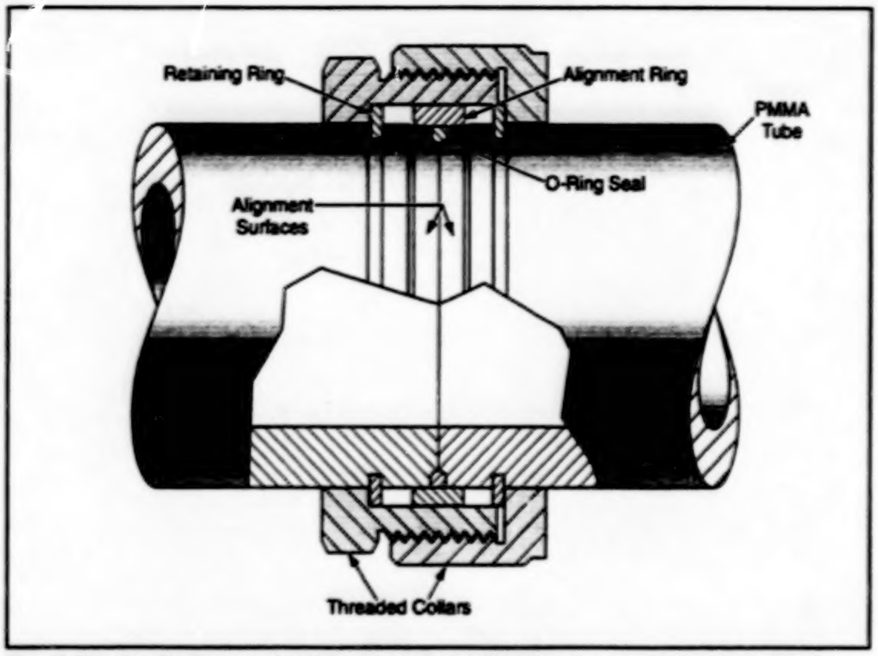

Two Tubes Are Sealed at a butt joint and held in alignment by a special coupling fixture.

The end surfaces of both tubes are machined flat and perpendicular to the inner surfaces. Cylindrical alignment surfaces referred to the inner surfaces are machined on the adjacent exterior end portions of the tubes. Facing halves of a seal groove are machined on the outer surfaces of the tubes at the butt joint. A retaining ring is placed in a groove on each tube at a short distance from the end. A male threaded collar is placed around one tube and a female threaded collar around the other tube, each collar covering and abutting the retaining ring on its respective tube.

The tubes are butted together along with an alignment ring and with an O-ring placed in the seal groove. The alignment ring is machined for a snug fit with the alignment surfaces on the tubes, thereby ensuring the precise alignment of the inner tube surfaces with each other. The two collars are threaded together until the force on the retaining rings pushes the ends of the tubes together. At this point, the O-ring is squeezed tightly between the tubes and the alignment ring, forming a tight seal.

In an alternative coupling scheme (not shown in the figure), the threaded collars are replaced by a combination of unthreaded collars and a two-piece ring clamp that engages the collars. The clamp features tapered surfaces that exert a longitudinal force to push the tubes together when the two halves of the clamp are bolted together.

This work was done by Robert Mate of the University of Houston for **Lewis Research Center**. *Further information is contained in a TSP [see page 1].*

Inquiries concerning rights for the commercial use of this invention should be addressed to NASA Lewis Research Center, Commercial Technology Office, Attn: Steve Fedor, Mail Stop 4-8, 21000 Brookpark Road, Cleveland, Ohio 44135. Refer to LEW-16255.

Equipping Quick-Disconnect Fittings To Detect Leaks

Quick-disconnect fittings on hoses and bellows can be equipped with sensors to detect leaks and misalignments that cause leaks. Experiments have shown that four types of sensors are effective for this purpose: force sensors, strain gauges, pressure transducers, and microphones. Of these, force sensors appear to be best for indicating misalignments. Microphones pick up the whistling sounds of gas leaks. Pressure transducers in purge cavities can indicate (a) increases in pressure that signify leaks in supply lines and (b) decreases in pressure that signify leaks in vent lines. The instrumented quick-disconnect fittings were conceived for use on the umbilical hoses used to supply gases and cryogenic liquids to spacecraft during preparation for launch. The concept also has potential for enhancing safety and helping to enable automation of fueling system for cars, trucks, buses, trains, and airplanes.

This work was done by Ronald L. Remus and Perry Hartford of Merritt Systems, Inc., for **Kennedy Space Center**.

Inquiries concerning rights for the commercial use of this invention should be addressed to the Technology Programs and Commercialization Office, Kennedy Space Center, (407) 867-6373. Refer to KSC-11893.

BLANK PAGE

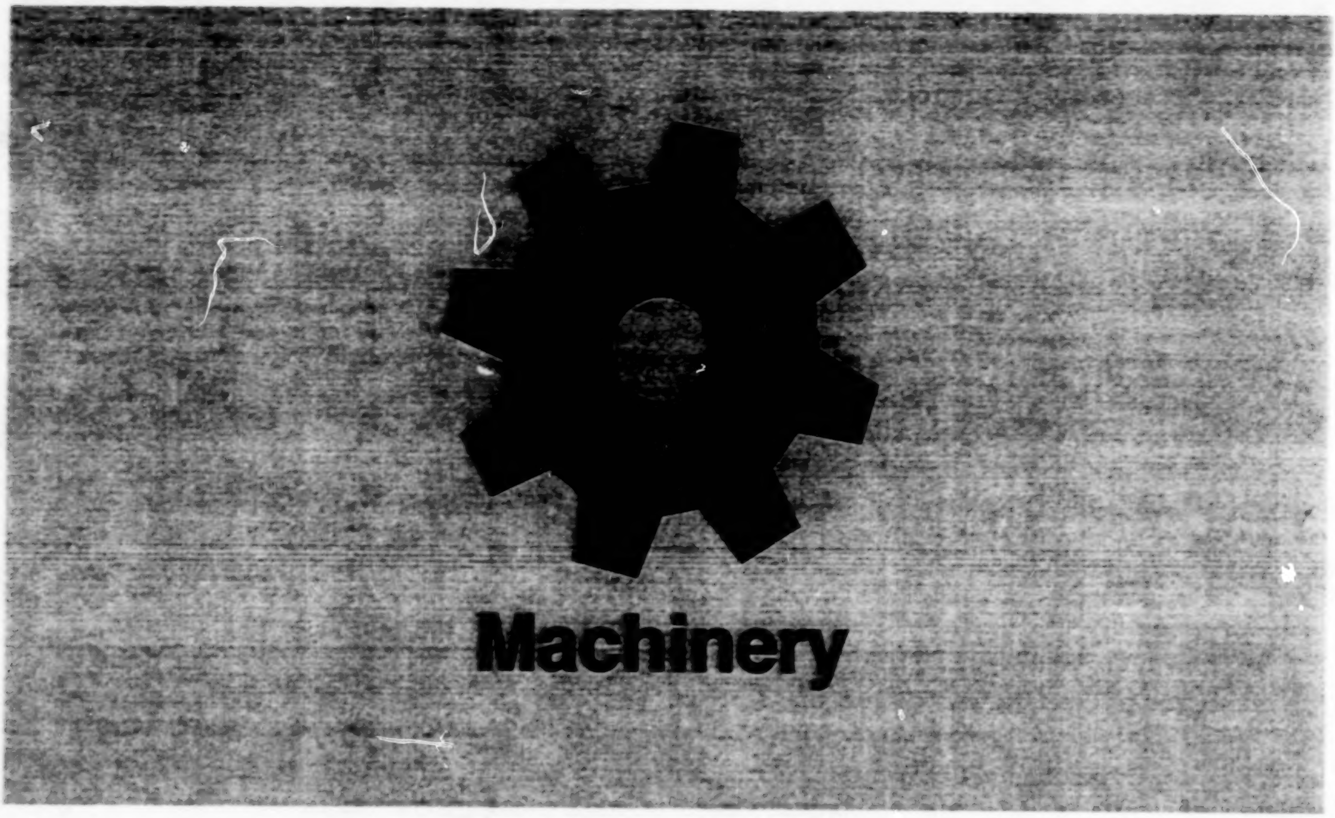

Hardware, Techniques, and Processes

BLANK PAGE

Ceramic Hybrid Electromechanical Systems

Mesoscopic ceramic-based devices would overcome key limitations of microscopic silicon-based devices.

NASA's Jet Propulsion Laboratory, Pasadena, California

Ceramic hybrid electromechanical systems (CHEMS) have been proposed to overcome some of the disadvantages while retaining most of the advantages of microelectromechanical systems (MEMS). Whereas MEMS are fabricated mostly by micromachining of silicon and have typical feature sizes of the order of microns or smaller, CHEMS could be fabricated on ceramic substrates by a wider variety of techniques and would have typical feature sizes ranging from tens of microns to millimeters. Depending on specific applications, CHEMS could serve as alternatives or complements to MEMS. CHEMS could be readily incorporated, along with integrated circuits and other microscopic components, into ceramic-based hybrid multilayer packages (e.g., multichip modules).

While the development of MEMS has been an important achievement in miniaturization, it turns out that in many practical applications, MEMS are too small to provide the required sensitivity as sensors or to provide the required forces or strokes as actuators. MEMS also suffer from stiction, squeeze-film damping, and damage induced by surface tension in liquids during processing. In addition, silicon is often not the substrate material of choice for applications in which there are requirements for electrically or thermally insulating substrates, low capacitance, resistance to corrosion, or hermetic sealing.

The proposal to develop CHEMS originated from the realization that many of the mechanical problems of MEMS could be solved more readily by fabrication of packaged microelectromechanical devices with dimensions intermediate between those of silicon-based microdevices and those of conventional macroscopic electromechanical devices. Sensors and actuators at the proposed CHEMS mesoscale could be made stronger and could be made to respond over dynamic ranges wider than those of silicon-based microdevices. Seals could be improved and strokes lengthened. Even so, CHEMS would still be small enough to fit into compact packages along with electronic integrated circuits.

In the development of CHEMS, it will be possible to take advantage of the mature technology already available for manufacture of ceramic hybrid structures in the electronics industry. There is an immense data base on ceramic materials with a wide variety of mechanical and electrical characteristics, including such sensor/actuator materials as piezoelectrics and ferroelectrics. Ceramic hybrids and multichip modules, and modern processes for manufacturing them, share many characteristics with those of silicon-based MEMS. Ceramic-hybrid technology affords the means to make laminated assemblies of ceramics, metals, and glasses that can be patterned, fired, and etched to produce three-dimensional structures. Inasmuch as silicon-based MEMS and electronic circuits are already typically integrated on ceramic substrates or headers, the fabrication of CHEMS should pose no obstacle to integration, nor should it entail additional cost. The completed systems would be of the same masses and volumes as those of

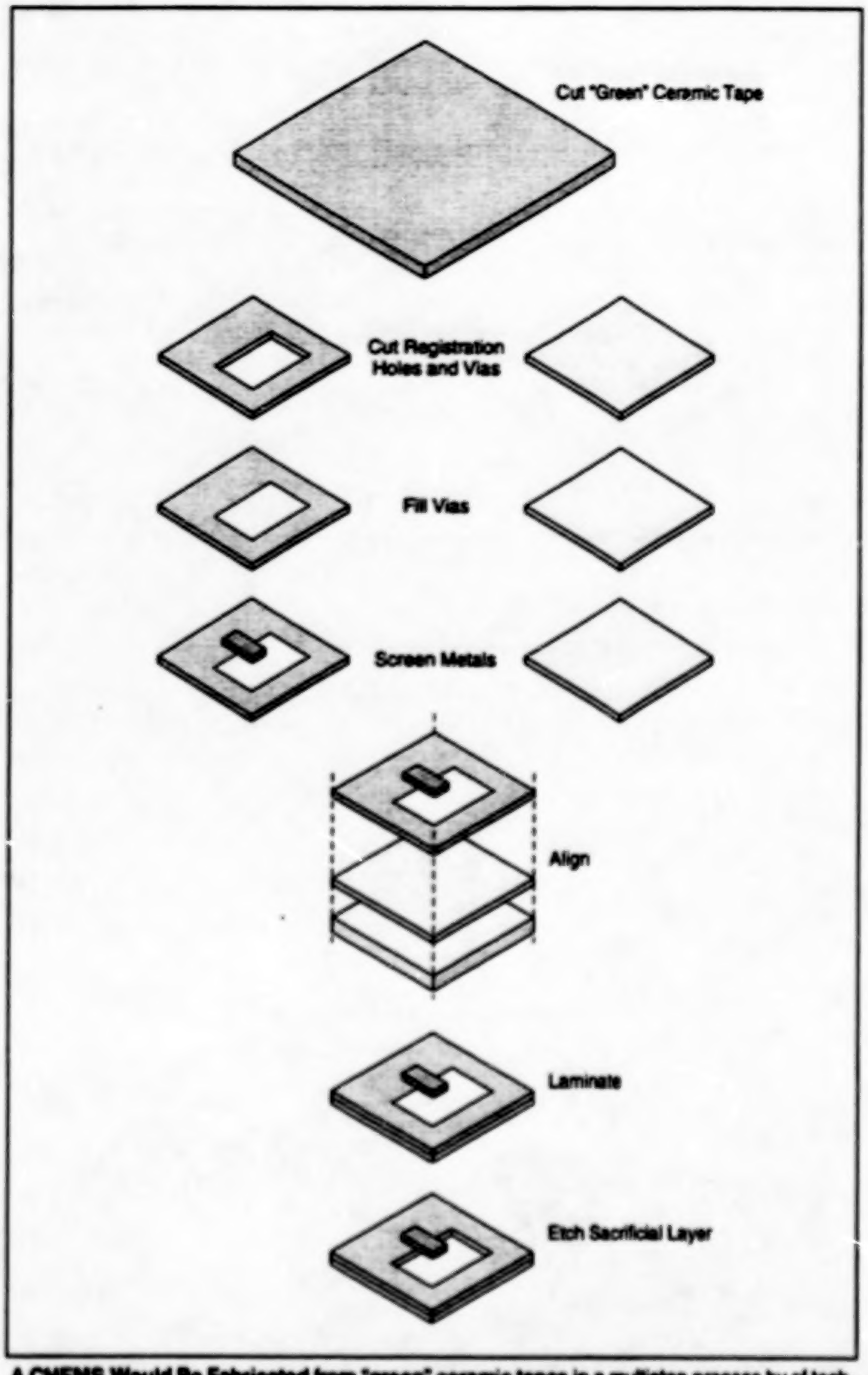

A CHEMS Would Be Fabricated from "green" ceramic tapes in a multistep process by of techniques that are established but have not been used to build devices of this type.

packaged silicon microfabricated devices, but would have greater capabilities because of the larger sizes of the active mechanical components.

The figure illustrates an example of fabrication of a multilayer CHEMS that would include a metal cantilever over a rectangular hole plus metal layers connected to each other electrically and mechanically. Fabrication would be accomplished by use of the low-temperature cofired ceramic (LTCC) process. The starting materials for the layers would be 250-μm-thick "green" (that is, not yet fired) ceramic tapes, typically composed of 40 to 60 percent Al_2O_3 and the balance of filler materials.

Via holes for mechanical registration and electrical contact would be stamped into the tapes by use of computer-aided design and automated cutting tools. The via holes for electrical connection would be filled with metal. The rectangular central hole would be filled with a sacrificial dielectric to support the cantilever to be formed in the next step. Metal layers would be screened onto the broad surfaces of the tapes, forming the cantilever among other metal features. The metal-patterned tapes would be stacked and aligned by use of pins through the registration holes. The stack would be laminated at a pressure of 3 kpsi (21 MPa) and temperature of 70 °C. Next, the laminated structure would be heated to 500 °C to drive out volatiles. The structure would be fired at 850 °C to set the ceramic. Finally, to free the cantilever, the sacrificial dielectric would be removed from the central rectangular hole by wet and/or dry chemical etching.

This work was done by Linda Miller, Michael Hecht, Martin Buehler, Amin Mottiwala, Beverly Eyre, and Indrani Chakraborty of Caltech for **NASA's Jet Propulsion Laboratory**. *Further information is contained in a TSP [see page 1].*

In accordance with Public Law 96-517, the contractor has elected to retain title to this invention. Inquiries concerning rights for its commercial use should be addressed to

Technology Reporting Office
JPL
Mail Stop 122-116
4800 Oak Grove Drive
Pasadena, CA 91109
(818) 354-2240

Refer to NPO-20356, volume and number of this NASA Tech Briefs *issue, and the page number.*

Wipers Based on Electroactive Polymeric Actuators

Advantages are simplicity and light weight.

NASA's Jet Propulsion Laboratory, Pasadena, California

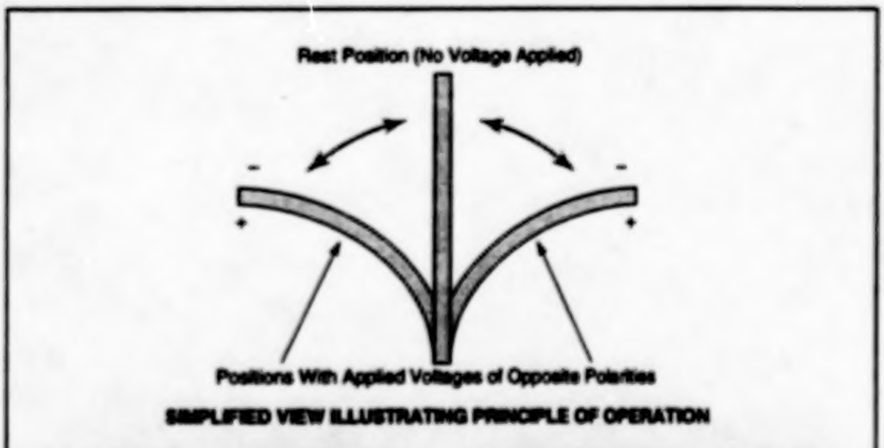

A Wiper Arm/Actuator Made of Ionomeric Film bends when a voltage is applied across its thickness. The direction of bending depends on the polarity of the voltage.

Wiping devices that exploit fingerlike bending motions produced by electroactive polymeric (ionomeric) actuators are undergoing development. These wiping devices function similarly to conventional windshield wipers. However, unlike conventional windshield wipers, these devices contain no motors, gears, or drive linkages; as a result, these devices are relatively simple, compact, and lightweight.

Conceived for use in wiping dust off solar cells and windows of scientific instruments to be sent to explore Mars, these wiping devices might be useful for similar purposes on Earth.

A device of this type is denoted by the acronym "SWEP" (for surface wiper actuated by electroactive polymers). The only moving part in a SWEP is the wiper arm/actuator. This part is made from electroactive polymers; namely, (a) a membrane made of an ion-exchange polymer sandwiched between (b) surface polymeric layers that contain or are coated with platinum and that serve as electrodes. When a small electric potential (typically a few volts) is applied to the electrodes, the sandwich bends. Depending on the magnitude of the applied voltage and the dimensions of the arm, the angle of bending could exceed 180°. The direction of bending depends on the polarity of the applied potential (see figure). Thus, one could make a wiper go back and forth across a surface, in the manner of a conventional windshield wiper, by applying an alternating voltage.

Electroactive polymers (EAPs) exhibit several characteristics that lend themselves well to SWEPs:

- EAPs can be mass-produced at costs much lower than those of piezoelectric materials, in large part because unlike piezoelectric materials, EAPs need not be poled.
- EAPs can readily be formed to

desired sizes and shapes.

- Physical characteristics of EAPs that are particularly well suited to actuation in SWEPs include high toughness, large electrostrictive strain, and inherent damping of vibrations.

Another advantage of SWEPs is low power consumption. For example, the prototype unit shown in the figure operates with a drive power of 20 to 30 mW. In a typical application, the frequency of the alternating driving voltage would be a fraction of a hertz; however, the frequency could be made higher if necessary, because the characteristic response time of a SWEP is of the order of milliseconds.

Like a conventional windshield wiper, a SWEP for a typical practical application would preferably be constructed as a wiper/actuator arm with a wiper blade or perhaps a brush attached. The shape, size, and material of the blade or brush could be chosen by design to minimize friction and ensure effectiveness in cleaning. As in the case of a conventional windshield wiper, the wiping should be done at the minimum frequency that provides effective cleaning, in order to minimize scratching.

This work was done by Yoseph Bar-Cohen and Tianji Xue of Caltech and Mohsen Shahinpoor of the University of New Mexico for **NASA's Jet Propulsion Laboratory**. *Further information is contained in a TSP [see page 1].*
NPO-20371

BLANK PAGE

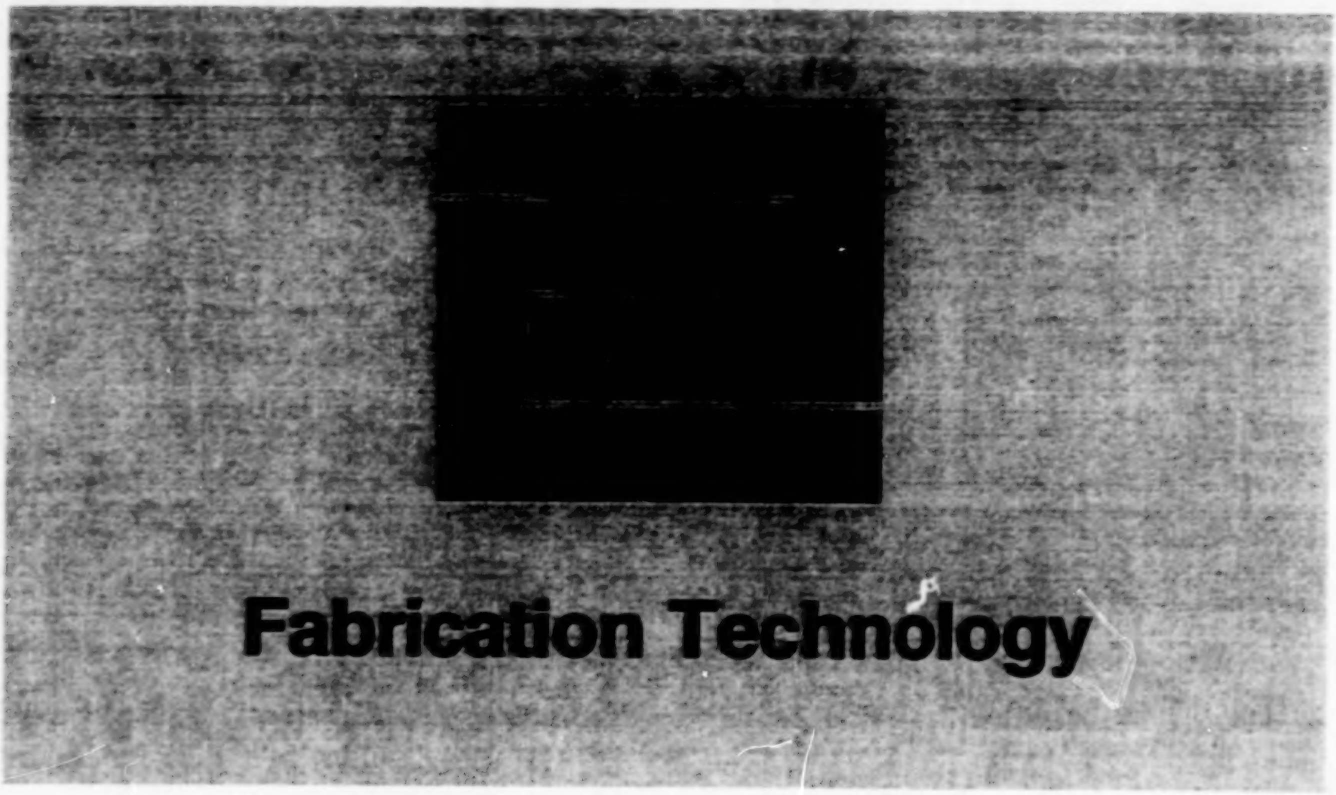

Fabrication Technology

Hardware, Techniques, and Processes

BLANK PAGE

52

Surface Micromachining of Diamond for Fabrication of MEMS Microstructures

Diamond bridges and cantilevers are formed by selective deposition and selective etching.

NASA's Jet Propulsion Laboratory, Pasadena, California

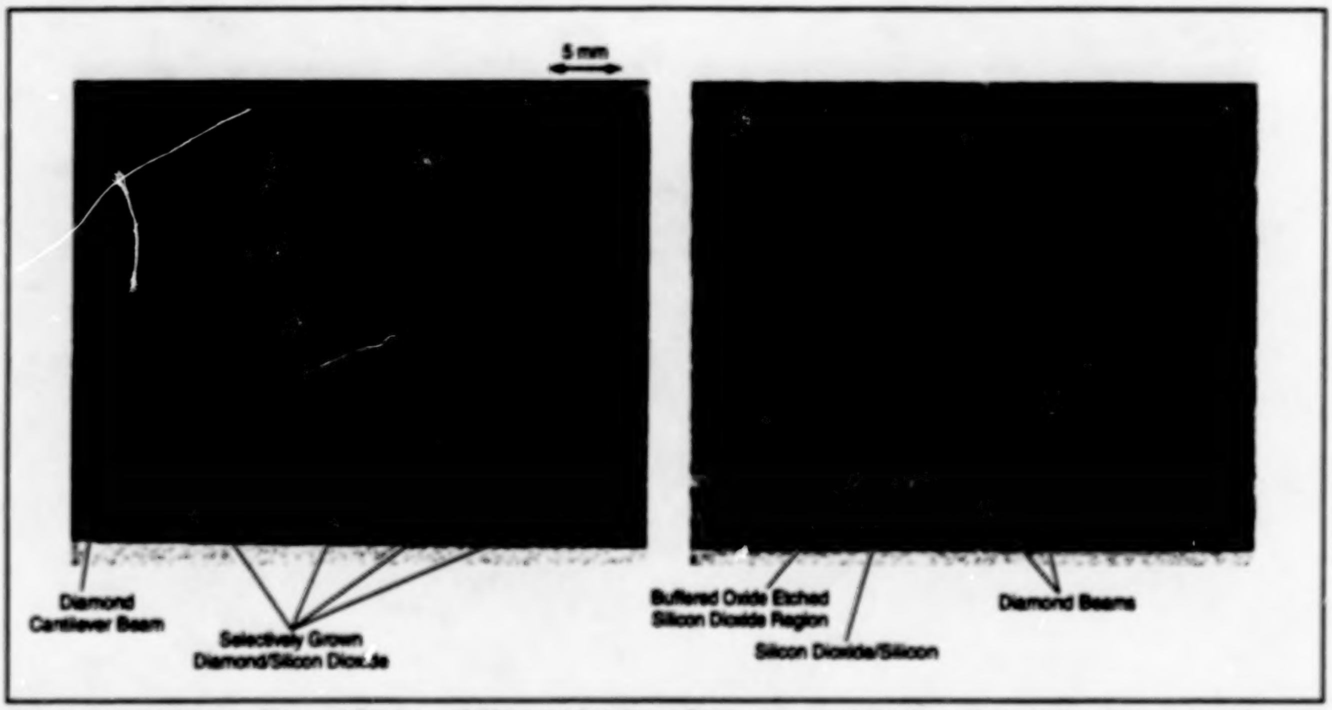

Optical photographs show **Diamond Beams and Diamond Cantilever Beams** that were fabricated using selective diamond deposition and subsequent micromachining process.

A surface-micromachining process has been devised for use in fabricating microscopic polycrystalline diamond structures (e.g., bridges and cantilevers) as integral parts of microelectromechanical systems (MEMS). The general concept of MEMS encompasses such diverse objects as simple mechanical actuators, simple mechanical sensors, or complex units containing electronic or optoelectronic circuitry integrated with mechanical sensors and/or actuators. Because diamond is highly resistant to corrosion and is transparent, the ability to form diamond structures could contribute to the development of MEMS to withstand corrosive environments. For example, diamond structures could serve as supports for corrosion-resistant electrodes in MEMS designed for biomedical applications. MEMS containing diamond films could also prove useful as automotive sensor and display devices.

An explanation of the distinction between surface and bulk micromachining is prerequisite to a description of the present diamond-surface-micromachining process. In bulk micromachining, three-dimensional features are etched into the bulk of a crystalline or noncrystalline material. In surface micromachining, features are built up, layer by layer, on a substrate of single-crystal silicon or other suitable material. The features in a given layer are defined by dry etching or selective deposition. Then the structure containing the feature is released from the substrate by wet etching (and consequent undercutting) of the substrate material.

The present diamond-surface-micromachining process is best described in terms of experiments in which it was first demonstrated. The starting substrates in the experiments were mirror-smooth, (100)-oriented single-crystal silicon wafers that were, variously, p- or n-doped to a resistivity <20 Ω·cm. The wafers were cleaned, then thermally oxidized to a depth of 1 to 1.5 micrometers.

Each substrate was prepared for selective deposition of diamond, following either procedure A or procedure B described below:

Procedure A. To increase the density of nucleation sites for diamond and thereby make it possible to obtain a pinhole-free diamond deposit, the surface of the oxidized substrate was damaged by ultrasonic agitation in methanol containing diamond particles. The ultrasonically damaged SiO_2 substrate surface was photolithographically patterned. By use of a buffered oxide-etch solution, the wafer was partially chemically etched through the openings in the photoresist to remove the damaged oxide surface layer and thereby define the areas where diamond was not to be deposited. The photoresist was then removed by commercial stripping solutions and the substrate cleaned in an oxygen plasma.

Procedure B. The SiO_2 substrate surface was photolithographically patterned, then the substrate was hard-baked at a temperature of 150 to 200°C. The substrate (with the photoresist still in place) was subjected to ultrasonic agitation in methanol containing diamond particles, so that the SiO_2 surface areas exposed through the holes in the photoresist mask would be damaged and would therefore become sites for deposition of diamond. Then the photoresist was stripped off and the substrate cleaned as in procedure A.

Following procedure A or B, the substrate was cleaned, then placed in a chemical-vapor-deposition (CVD) chamber. Polycrystalline diamond was grown on the patterned and damaged SiO_2 areas by CVD from a flowing mixture of methane and hydrogen, typically at a total pressure of 45 torr (6 kPa) and a substrate temperature of 950 °C.

The diamond-patterned substrate

was cleaned in solvents. In a photolithographic process, a new photoresist pattern was formed to define the portions of the substrate to be etched away from the diamond. Then by use of a buffered oxide-etch solution, the SiO_2 layer on the substrate was removed from under selected diamond-patterned areas, leaving diamond structures supported over airgaps (bridges and cantilevers).

This work was done by Rajeshuni Ramesham of Caltech for **NASA's Jet Propulsion Laboratory**. *Further information is contained in a TSP [see page 1].*
NPO-20529

Mathematics and Information Sciences

Hardware, Techniques, and Processes

BLANK PAGE

56

Software for Developing Autopilots for Launch Rockets

User-friendly software would accelerate development and promote safety.

American GNC Corporation, Chatsworth, CA

Three integrated software products are being developed for use in the further development of autopilot systems for reusable launch vehicles (RLVs). The need for these products arises because of the unique nature of RLVs:

- RLVs employ differential throttling as the primary means of longitudinal control during ascent. This approach to flight control necessitates autopilot systems because the way in which engine thrust signals control the rockets is counterintuitive to astronauts.
- Conventional controllers are not adequate for the multiple-input/multiple-output autopilot systems that are needed for RLVs (e.g., the VentureStar) that are equipped with linear aerospike engines and small conventional aerodynamic controls. The small conventional aerodynamic controls and the propulsion inefficiency that results from differential throttling necessitate the development of robust reconfigurable autopilot systems, as do the all-consuming goal of minimizing RLV weight and the need for interchangeable, swappable, and cooperative actuators that can alleviate attitude-control concerns in the event of single or multiple actuator failures.

One of the three developmental software products is intended for use in designing and simulating autonomous, robust, reconfigurable flight-control systems of both civil and military RLVs. This is a user-friendly software package that will greatly aid NASA, other government agencies, and industrial organizations working on linear aerospike space transportation systems and RLVs. It enables the designer to develop systems based on several control approaches, including hierarchical robust reconfigurable control and robust identification-based adaptive reconfigurable control. Genetic algorithms serve as the optimization tools in this package.

The second software product is one that provides an advanced software environment of testing and evaluation of the designs and software of autopilot systems. This product will determine the efficacy of these systems by evaluating the ease with which the systems can be reconfigured in the event of the multiple failure scenarios described below.

The third and final product is a real-time software prototype of an advanced robust reconfigurable autopilot system for an RLV. It is an on-line, real-time control software environment that provides control researchers and engineers with a convenient tool for the investigation and application of advanced control methods and real-time control in an RLV system.

The advantages of these three integrated software products and of autopilot systems designed by use of them are the following:

- These products will minimize the engineering design labor as well as the weight, cost, labor, and maintenance associated with the physical RLV.
- Autopilot designers will be able to design, simulate, evaluate, implement (in real time), and test their control system designs within the complete three-product package.
- A robust, reconfigurable autopilot eliminates the need for a human pilot, thus eliminating the possibility of loss of life as the result of a catastrophic failure or human error.
- The use of software products like these reduces the probability of losing an RLV and/or its payload in the event of a mission-threatening failure. A robust, reconfigurable autopilot system would minimize the need to abort the mission in the event of a single or multiple actuator failure by reconfiguring the RLV control system as necessary to approach nominal vehicle attitude control.
- In designing a robust, reconfigurable attitude-control system, the control actuators can be allowed to remain small, minimizing the vehicle weight and avoiding actuator-related overheating during reentry and descent.
- To minimize weight, a typical RLV design calls for fuel for both the main engines and the reaction control system to be depleted before descent. Thus, the need for reconfigurability of aerodynamic control surfaces becomes even more compelling during descent and landing in the event of a single or multiple aerodynamic actuator failure.

This work has been and will be undertaken by the **American GNC Corporation**, *9131 Mason Avenue, Chatsworth, CA 91311, an SBA 8(a) certified Small Disadvantaged Business concern, as part of a NASA Small Business Technology Transfer (STTR) project monitored by* **Marshall Space Flight Center**. *The NASA STTR Contract Number is NAS8-97292; Topic: 5; Topic Title: Advanced Space Transportation. For further information, contact Dr. Ching-Fang Lin, (818) 407-0092 or e-mail: cflin@americangnc.com.*
STTR0001

National Aeronautics and
Space Administration

NASA

58

END

04\23\99